University of Southern Queensland

Faculty of Health, Engineering and Sciences

Development of a computer simulation for scouring around bridge piers

A dissertation submitted by

Gary A. Nankervis

in fulfilment of the requirements of

ENG4111 and ENG4112 Research Project

towards the degree of

Bachelor of Engineering (Honours) (Civil)

Submitted October, 2016

Abstract

Bridges are important and valuable items of infrastructure in modern society. They are designed to be functional and cost effective, but they must also be safe. A great many bridges cross bodies of flowing water and have supporting piers founded within the water; therefore the foundations are subject to erosion by scouring and this could lead to potential bridge failures.

The aim of this research project is to develop a computer simulation of bridge pier scouring, to accurately predict the extent of potential scouring. Accurate predictions of scouring could lead to more efficient bridge designs while still maintaining the required level of safety. The project also proposes a new pier design with potential for improved scouring performance.

There has previously been much research conducted on various aspects of bridge pier scouring. This includes explaining the scouring mechanism, physical experiments on pier geometries and developing prediction formulas. Most of this work has been done using scale models in a hydraulic flume tank and therefore has some limitations in transference to real scale situations.

In recent years computer simulations have been developed for bridge pier scouring. They have an advantage of being able to model a situation at real scale, and can easily be altered as required. Early simulations were mainly single-phase (one fluid; water) models which require empirical sediment transport equations to predict sand movement. Multiphase (more than one fluid) simulation models are a more recent development; they model sediment transport as a granular flow.

In this project Computational Fluid Dynamics (CFD) was used to develop the simulation model in ANSYS Fluent, which is a commercial software package. The model is a three-dimensional multiphase model with sand and water phases. It was based on a cylindrical control pier in a previous experiment so that known results

could be used to validate the model. A new streamlined slotted pier geometry was proposed for performance testing with the model after validation.

At present, development of the model does not achieve the anticipated objective of simulating local scouring around a bridge pier. The simulation of sand, as a riverbed sediment, is not realistic. Therefore the model has not been validated and is not reliable. The sand appears to behave much more like a liquid rather than a semi-solid granular flow.

The new pier design when tested in a two-dimensional (horizontal plane) model shows potential for reduced scouring. This is because of lower water velocity along its outer edges, compared to the cylindrical control pier. However it has not been possible to test the new pier in a three-dimensional scouring model.

Future successful development with this simulation model is dependent on further research and experimentation to achieve realistic sand movement. Additional models would be required specifically to better understand modelling of sand flow and the most appropriate parameter choices to achieve it.

Results from this project may offer some useful insights to other researchers, or ideas for future research projects.

University of Southern Queensland

Faculty of Health, Engineering and Sciences

ENG4111/ENG4112 Research Project

Limitations of Use

The Council of the University of Southern Queensland, its Faculty of Health, Engineering & Sciences, and the staff of the University of Southern Queensland, do not accept any responsibility for the truth, accuracy or completeness of material contained within or associated with this dissertation.

Persons using all or any part of this material do so at their own risk, and not at the risk of the Council of the University of Southern Queensland, its Faculty of Health, Engineering & Sciences or the staff of the University of Southern Queensland.

This dissertation reports an educational exercise and has no purpose or validity beyond this exercise. The sole purpose of the course pair entitled "Research Project" is to contribute to the overall education within the student's chosen degree program. This document, the associated hardware, software, drawings, and other material set out in the associated appendices should not be used for any other purpose: if they are so used, it is entirely at the risk of the user.

University of Southern Queensland

Faculty of Health, Engineering and Sciences

ENG4111/ENG4112 Research Project

Certification of Dissertation

I certify that the ideas, designs and experimental work, results, analyses and conclusions set out in this dissertation are entirely my own effort, except where otherwise indicated and acknowledged.

I further certify that the work is original and has not been previously submitted for assessment in any other course or institution, except where specifically stated.

Gary Nankervis
Student Number: 0050083838

Acknowledgements

I would like to thank my project supervisor, Dr Andrew Wandel. His knowledge of the software package and advice on implementing it have been invaluable.

I would also like to thank my family. Their understanding and support throughout my studies and this research project are greatly appreciated.

Table of Contents

List of figures

List of Tables

Nomenclature

Note: depending on original document sources, a symbol may sometimes be used to represent different parameters, or alternatively different symbols may sometimes be used to represent the same parameter.

2-D	Two dimensional.
3-D	Three dimensional.
d_{50}	Sediment particle diameter at 50 percentile of a given range.
d_{84}	Sediment particle diameter at 84 percentile of a given range.
CFD	Computational Fluid Dynamics.
D	Diameter, in general usage.
D	Pier width (equivalent diameter), used in the Melville equation.
D_{50}	As for d_{50}, but specifically used in the Sheppard equation.
g	Gravitational acceleration, taken as 9.81 m s^{-2} .
k	Unit multiplier, equal to 1000.
u	Velocity
U	Velocity
UDF	User defined function.
V	Velocity
V_f	Volume fraction.
y, or y_0	Normal flow depth, unaffected by any flow obstruction.

Glossary of terms

Bed load;

Sediment grains roll, or are dragged, across the stream bed surface but are not lifted into suspension.

Clear-water transport;

There is no sediment transport already coming from upstream.

Live-bed transport;

There is already incoming sediment transport which originated further upstream.

Multiphase flow;

Two or more fluids flowing within the same volumetric space.

Packing limit;

The maximum volume of a granular phase material which can be packed into a volume space, expressed as a proportion. (Takes account of void space).

Suspended load;

Sediment grains are lifted into suspension and carried by the fluid flow.

Volume fraction;

The proportion of a volume space occupied by a particular secondary phase material.

Chapter 1

Introduction

The research project is focused on scouring around bridge piers. It aims to improve the safety and cost efficiency of future bridges by developing an accurate computer simulation model for predicting the extent of scouring around bridge piers.

The dissertation provides a background to the scouring problem, sets out the project aims, examines previous research on the problem, explains project development methodology and presents project results.

1.1 Background

As part of a nation's road and rail infrastructure, bridges provide a means of easy and efficient access to cross barriers like waterways, gorges and other un-trafficable areas. Bridges have considerable economic and social value in allowing personal travel and transport of goods. The failure of a bridge therefore imposes a significant cost on society, not just in monetary terms but perhaps also in loss of life.

The American Federal Highway Administration (FHWA) has found scouring to be a significant contributing factor in many bridge failures (Arneson et al. 2012), therefore, during bridge design there is need for accurate prediction of potential scouring effects. Historically scour estimation was based on designer's experience, but later evolved to experimentally-based prediction equations. Computer simulation modelling could provide a better means to study and more accurately predict the extent of scouring.

Scouring is generally defined as erosion of stream bed material, under the influence and power of flowing water (Arneson et al. 2012). It can undermine the structural integrity of bridge foundations, potentially leading to bridge failures.

Scouring is a dynamic process which can occur in several different forms (Arneson et al. 2012), either alone or in combination. General scour can occur anywhere along the length of a riverbed, contraction scour occurs adjacent to a flow restriction, and local scour occurs surrounding particular flow obstructions. Only local scour around bridge piers is considered in this research project. Figure 1.1 shows a very prominent example of local scour.

Figure 1.1 Local scour around a bridge pier (FDOT 2005).

1.2 Project aims

This research project aims to:

- Develop a three-dimensional, computational fluid dynamics (CFD) model for simulating water flow and river bed scouring around bridge piers.
- Enable more accurate prediction of scouring around new and novel bridge pier designs, at the design stage.
- Critically examine an alternative bridge pier design using the model.

The project aims and objectives are listed in the project specification which is attached as Appendix A.

1.3 Specific objectives

1. Conduct a literature search and review to discover existing knowledge and background information relating to bridge failure, the scouring process, and CFD modelling techniques. This will help identify a starting point based on extending the existing knowledge, and to identify gaps in the existing knowledge.
2. Propose a new and novel pier geometry based on existing knowledge of the scouring process, and as an extension of previously trialled pier geometries. The shape of the new design is expected to produce lower flow velocities around the pier, and therefore should also cause reduced scouring.
3. Develop a 2-D single-phase steady-state model to analyse water flow velocities. This is a relatively simple form of model which will not consume excessive computational runtime, but is quite adequate to examine flow velocities. Velocities around a traditional cylindrical pier are to be examined to establish a benchmark for comparison with those of a new and novel pier geometry. Reduced flow velocity around the new pier would prove it has potential to reduce scouring.
4. Further develop the model into a two-phase transient model. This more complex form of model is required to examine the inter-related flow of two different materials (phases) over a long time period. Granular river bed material is considered as a secondary phase fluid which moves (flows) as a consequence of the primary phase fluid (water) flow. The more complex model will have a much longer computational runtime.
5. Validate and/or calibrate the model against pre-existing experimental results by replicating all the parameters of a benchmark experiment involving circular piers. Accurate model results are dependent on correct choice of input parameters, values and techniques, therefore testing the model against a set of known results is essential to verify the model performs correctly. If the model does not perform correctly it may need to be calibrated by adjusting specific parameters until the correct results are achieved. A sensitivity analysis may also be required to see which parameters have the most significant effect on results.

6. Use the two-phase model to test scouring around the new pier design. This is the practical application of the model to test performance of a new pier design.
7. Compare modelling results with traditional scour estimates based on empirical formulae. This comparison checks for similarity or difference between results. Results will be examined and discussed in order to conclude whether the modelled results can be considered more accurate or not.

As time and resources permit:

1. Trial and evaluate different geometric variations. Once the model has been created it can easily be rerun with other variations of pier geometry to see if performance can be further improved.
2. Trial and evaluate different flow approach angles. The new pier design proposed in this research may not perform as well with increasingly oblique flow approach angles. Therefore different approach angles should be tested to see if performance is reduced or not.

1.4 Consequential effects

Positive effects of the project are an increase of knowledge on the subject of developing computer simulations to predict bridge pier scouring. If further development work can produce an accurate model, then application of the model could lead to more cost-efficient bridge designs which still provide satisfactory structural integrity.

Results of this research project may be of future benefit for further model development. Additional research and experimentation may be able to improve the model.

Chapter 2

Background and Literature review

This chapter reviews the available literature, from textbooks or previous research, related to the aims of this project. It identifies existing knowledge/information which may be useful to this project, and also identifies areas where there may not be sufficient existing knowledge.

2.1 Bridges

2.1.1 Bridge and pier design

Many bridges use multiple simply supported spans to achieve the required total span length (Fu 2013). This design requires supporting piers, at the end of each span, founded on piles or spread footings. The piers may consist of a single, or multiple, columns. Multiple columns are usually interconnected at the top by a pier cap, with the bottoms either independent or interconnected by a footing. Column cross-sections are usually circular, square, or rectangular; they may also have rounded or angled ends to assist streamlining of water flow. Some long length piers may take the form of a continuous wall, rather than multiple columns.

When crossing waterways, piers must be founded within the riverbed, and are vulnerable to scouring.

Bridge designers need to optimise their designs (Fu 2013) in order to provide structural integrity under adverse circumstances, while also achieving a cost effective structure. To design the minimum satisfactory foundation designers need an accurate prediction of maximum scour depth expected throughout the lifetime of the bridge.

2.1.2 Failure causes

A study of 114 reported bridge failures in the United States of America (Harik et al. 1990), between 1951 and 1988, categorised the causes of failure. Loss of use in at least one traffic lane was considered as a failure, and the worst case scenario was total collapse. The study authors suggest failures with potential for loss of life should be considered unacceptable, and designers should endeavour to prevent them. Accordingly the study was a first step towards developing a database of bridge failure details in order to improve future bridge design and construction.

The Harik et al. (1990) study was based on reports published in the public media; therefore it may not have included all bridge failures during the period. The accuracy and level of detail reported by these sources was limited. The study found natural phenomena to be the second most significant cause of bridge failures, after collisions from ships/vehicles. Natural phenomena included such things as floods, scouring and wind. Results could not be quantified any more accurately because detailed investigation records did not exist.

Wardhana and Hadipriono (2003) conducted a more comprehensive study of 503 bridge failures between 1989 and 2000. During this period the New York Department of Transport (NYDOT) made an effort to collect and record relevant details from bridge failure incidents throughout the United States, but not all states supplied information. Most failure details for this study were obtained from the NYDOT database, however some supplementary information was from other published reports. The study concluded 48% of failures were attributed to flooding and scouring. The authors suggest these two closely related causes may actually be the same thing but described differently by the different people reporting the incidents.

2.2 The scouring process

2.2.1 Characteristic flow

The characteristic nature of a fluid flow may be laminar, transitional or turbulent. The Reynolds Number (*Re*) is a dimensionless number used to determine the characteristic nature of a flow, and to compare the nature of one flow with that of others. Results are indicative only, with lower values suggesting laminar flow and higher values suggesting turbulent flow. By comparison with commonly accepted reference values, the calculated result is used to indicate if a particular flow situation is likely to be laminar, transitional, or turbulent. Reynolds Number is calculated from the formula

$$Re = \frac{\rho VD}{\mu} = \frac{VD}{\nu}, \qquad (2.1)$$

where ρ is fluid density, *V* is flow velocity, *D* is diameter (characteristic length dimension), μ is dynamic viscosity, and ν is kinematic viscosity (Chadwick et al. 2004).

The Reynolds number is usually used in relation to flow through pipes but by substituting different characteristic lengths the formula can be used for flow through channels, flow around bodies (e.g. Piers) or flow around particles (e.g. Sediment or gravel) (Nalluri & Featherstone 2001). In the different situations, the characteristic length values are likely to be in different ranges of magnitude therefore the accepted reference values to distinguish between laminar and turbulent flow also differ.

This project is concerned with flow through open channels (e.g. riverbeds), and flow around bodies (e.g. piers). For open channel flow, hydraulic radius (*R*) is used as the characteristic length, rather than the diameter as used for pipes. Furthermore, where a channel flow is considerably wider than it is deep, the hydraulic radius is approximately equal to depth, therefore depth can be used as a simplification. For flow around bodies, the body diameter (or an equivalent approximation) is used as the characteristic length.

For practical purposes, water flow in open channels and around submerged bodies is nearly always turbulent (Chadwick et al. 2004).

2.2.2 Sediment transport

Natural riverbeds generally consist of sediment particles which vary in size, shape and composition. Some of these particles may be dislodged, by the force of flowing water, and migrate downstream (Nalluri & Featherstone 2001). Such particle movement is known as sediment transport. Sediment transport can occur as "bed load", or "suspended load" (Chadwick et al. 2004). The two transport modes can occur simultaneously.

Bed load occurs when individual particles either slide or roll along the bed surface (Chadwick et al. 2004). For this to happen, water forces acting on each particle must overcome the critical shear stress which exists between particles and the river bed. Smaller and lighter particles have a lower value of critical shear stress so they require less force to move and will be first to migrate.

Suspended load occurs when turbulent water flow happens to act in a direction which imparts an uplift force component on particles (Chadwick et al. 2004). If the uplift force overcomes the gravitational force, particles are lifted up off the riverbed and become suspended in the water flow. Smaller and lighter particles are also more prone to this transport mode than larger particles.

Sediment transport can occur under "clear water" or "live bed" conditions (FDOT 2005). Clear water transport is when there is no sediment already coming from further upstream; only local scour occurs, and sediments are redeposited just downstream of the flow obstruction. Live bed transport is when sediment from scouring further upstream is already moving downstream. This means a local scour site will have sediment being transported in to the scour site as well as local sediment being transported out. A scour hole develops when transport out exceeds transport in. Under live bed conditions, a scour hole may be refilled to some degree

by upstream sediment inflow. This is not a solution to the scouring problem because it is only loose fill, and not firmly packed as the original stream bed would have been.

For a given riverbed, under normal flow conditions, all of the smallest particles, which may have once been present, will have been completely transported away. Of the particles remaining, the smallest size is related to flow velocity and is determined from the critical shear stress. The condition whereby there are no particles smaller than a certain size is known as “bed armouring” (Chadwick et al. 2004).

In stream flow where the bed is significantly wider than flow depth, bed shear stress (τ_b) can be taken as equal to mean shear stress (τ_0), and hydraulic radius (R) can be taken as equal to flow depth (y_0). At the threshold of particle motion, particle critical shear stress (τ_{cr}) is equal to average bed shear stress:

$$\tau_{cr} = \tau_0 = \rho g y_0 S_0 \,, \tag{2.2}$$

where,

ρ is fluid density,

g is gravity, and

S_0 is bed slope.

Critical friction velocity (u_{*c}) is a theoretical reference value derived from the bed shear stress:

$$u_{*c} = \sqrt{\tau_0/\rho} = \sqrt{g y_0 S_0} \,. \tag{2.3}$$

The entrainment function (F_s) (Chadwick et al. 2004) is used with the Shields diagram to determine whether particle motion will occur or not.

$$F_S = \frac{\tau_{CR}}{(\rho_S - \rho) g D} \,, \tag{2.4}$$

where,

ρ_s is sediment particle density,

D is particle diameter.

The Shields diagram, shown in Figure 2.1, plots the entrainment function against a form of Reynolds number, known as the shear Reynolds number (Re_*). The shear Reynolds number uses friction velocity (u_*) as the fluid velocity term.

$$Re_* = \frac{u_* D}{v} \tag{2.5}$$

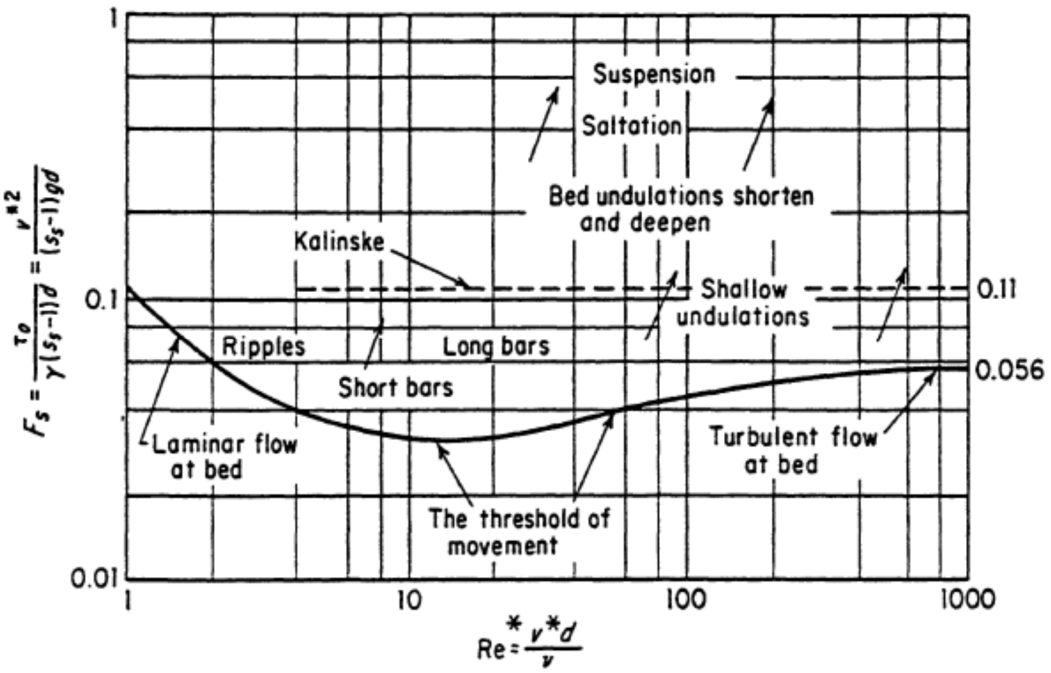

Figure 2.1 The Shields diagram plots entrainment function against the shear Reynolds number to indicate threshold of motion (Henderson 1966).

The curve plotted on the Shields diagram is known as the Shields function. It indicates the threshold of particle motion. Co-ordinates of entrainment function and shear Reynolds number which plot below the Shields function will be stable, whereas those which plot above the function will be dislodged.

For an experimental study of local scouring, comparison of particle critical shear stress with mean bed shear stress is important to ensure sediment transport is not likely to occur under normal flow conditions; that would constitute general scouring rather than local scouring.

2.2.3 Local scouring mechanism

Local scour occurs around an obstruction in the path of fluid flow. The obstruction forces the flow to divert its path in order to get past the obstruction. A cylindrical pier is commonly used as a benchmark in flow experiments and analysis (Zevenberger 2005) because it is a simple, yet realistic, geometric shape. Figure 2.2 shows typical disturbances to the flow around a cylindrical pier.

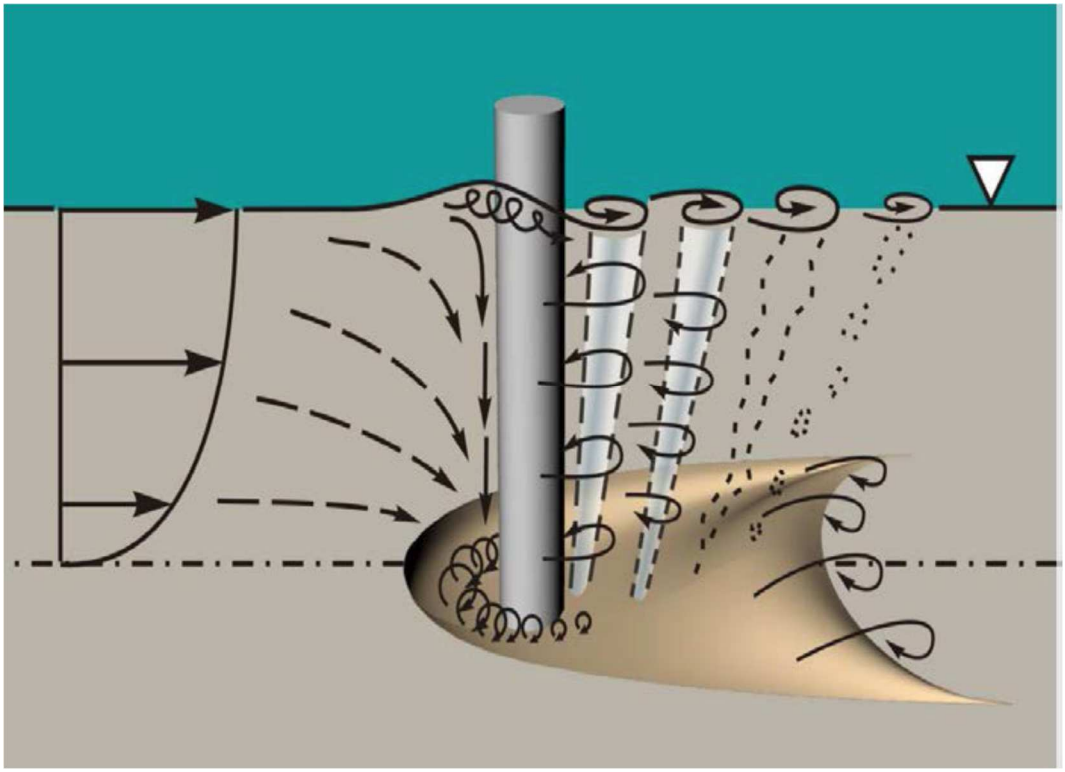

Figure 2.2 Flow disturbance around a cylindrical pier (Arneson et al. 2012).

The scouring mechanism was described by Laursen and Toch (cited in Melville 1975). A vertical profile of normal unobstructed flow velocity, shown at left in the

diagram of Figure 2.2, approaches the pier from upstream. Free flow and maximum velocity occurs near the water surface, while least velocity occurs near the stream bed due to surface friction causing an energy loss in the boundary layer. As the vertical velocity profile reaches, and is obstructed by, the front (nose) of the pier a high pressure region develops. A pressure gradient forms with higher pressure near the water surface and reducing to lower pressure near the stream bed.

Oncoming flow attempts to divert to areas of lower pressure. Near the surface, a small upwelling occurs, but beneath the surface, flow is diverted down the face of the pier toward the stream bed (Laursen and Toch cited in Melville 1975). When obstructed again by the stream bed, this flow is diverted upstream along the stream bed and towards the oncoming normal flow. This is the start of a vortex in front of and at the base of the pier.

High pressure at the front of the pier simultaneously seeks to divert flow to lower pressure areas around the sides of the pier. The vortex formed in front of the pier is swept around the sides of the pier in a spiralling manner (Laursen and Toch cited in Melville 1975). The result is called a horseshoe vortex due to its characteristic shape.

All of the previously obstructed flow ultimately has to divert around the pier. This causes an increased flow rate through a now constricted cross-sectional area, therefore flow velocity increases around the pier in accord with the conservation of mass theory.

High and/or increased flow velocity around the pier causes a shearing action at the pier wall boundary layer. A vertical wake vortex forms on each side of the pier, spiralling into the low pressure area directly behind the pier (Laursen and Toch cited in Melville 1975). These wake vortices periodically shear away and travel downstream with the flow. They are known to contribute to local scouring downstream of the pier, however they will not specifically be considered in this research project.

At the bed surface, increased turbulence due to the horseshoe vortex and increased flow velocity around the sides of the pier cause local scouring. In this region, larger sediment particles can be transported away downstream, compared with normal flow velocity over the general bed surface. Scouring starts as a small depression on each side of the pier, then grows into larger holes which migrate upstream until both sides meet at the nose of the pier (Melville 1975). Once started, scouring continues until an equilibrium state is achieved (Melville 1975) whereby the scour hole is large enough to allow flow to divert around the base of the pier without increased velocity adjacent to the modified bed surface.

2.3 Previous bridge scour research

From the 1950's, and up to the present day, considerable research has been conducted with regard to scouring at bridge sites. Researchers are usually from university engineering departments, or government road authorities; sometimes working collaboratively.

Several researchers and organisations are quite prominent in the literature over several decades. They are:

- E.V. Richardson and S.R. Davis, Colorado State University (CSU),
- D. M. Sheppard, University of Florida,
- B.W. Melville, Auckland University,
- American Federal Highway Administration (FHWA), and
- Florida Department of Transport (FDOT).

The researchers named above have each developed their own equations for prediction of maximum scouring depth, and these are three of the most commonly used prediction equations (Zevenberger 2005).

Past research has generally been conducted as experiments using scale models in a flume tank (FDOT 2005). There are a number of limitations imposed on these experiments, therefore they cannot accurately represent realistic situations. Experiments are usually conducted with uniform water flow, constant water depth, homogenous close graded cohesion-less bed material (sand), clear water transport

conditions, flat bed and side walls of virtual channel, and scaled pier models. In reality bedding materials are inconsistent and flow is unsteady, rising to a peak then falling again. This leads to clear water transport followed by live bed transport, then back to clear water transport.

Previous research has examined characteristics of water flow and turbulence, the mechanism of riverbed scouring, bridge pier geometry, and performance of scouring countermeasures. Countermeasures are either flow altering devices or riverbed armouring devices.

Early experiments were based on cylindrical piers only. Later experiments often introduced some sort of geometric variation, as a scour reduction countermeasure, and compared performance with that of a cylindrical reference pier.

2.3.1 Melville experiment

Melville (1975) conducted cylindrical pier scour experiments in a flume tank at the University of Auckland. The main aim, at that time, was to better understand the scouring mechanism, rather than predict the scour depth. The research built on an earlier understanding of the scouring process by Laursen and Toch (1956). Melville commented that the flume could not perform live bed transport experiments because it did not have sand feed and collection (cycling) capability, however maximum scouring was expected to be at threshold conditions. Results were presented as a contour map and tabular data of the scour holes. A revised understanding of the scouring process was also discussed.

The experiment and results were well documented, and often cited by other subsequent researchers. The results are often used as a benchmark to verify the results of more recent experiments, particularly those from numerical modelling.

This research project also uses the Melville (1975) experiment as a benchmark for validation. A contour plot of the resulting equilibrium scour hole is shown in Figure 2.3, and further results are attached in Appendix B.

The CFD model will, as far as practicable, be run using all the same parameters as the Melville experiment.

The Melville (1975) experiment parameters are:

- Flume = 45.6 cm wide x 44 cm deep x 19 m long. 12.7 cm false floor depth. Glass panel sides.
- Bedslope (S_0) = 0.0001 m/m.
- Flow depth (y_0) = 15 cm.
- Pier = 5.08 cm diameter (1/9 width ratio).
- Sand d_{50} = 0.385 mm, ρ_s = 2650 kg/m^3, 32° angle of repose.
- Inlet mean velocity (V_0) = 0.25 m/s. Discharge (Q) = 17.12 L/s.
- Bed shear velocity (u_*) = 0.0121 m/s.
- Critical particle shear velocity (u_{*cr}) = 0.014 m/s.

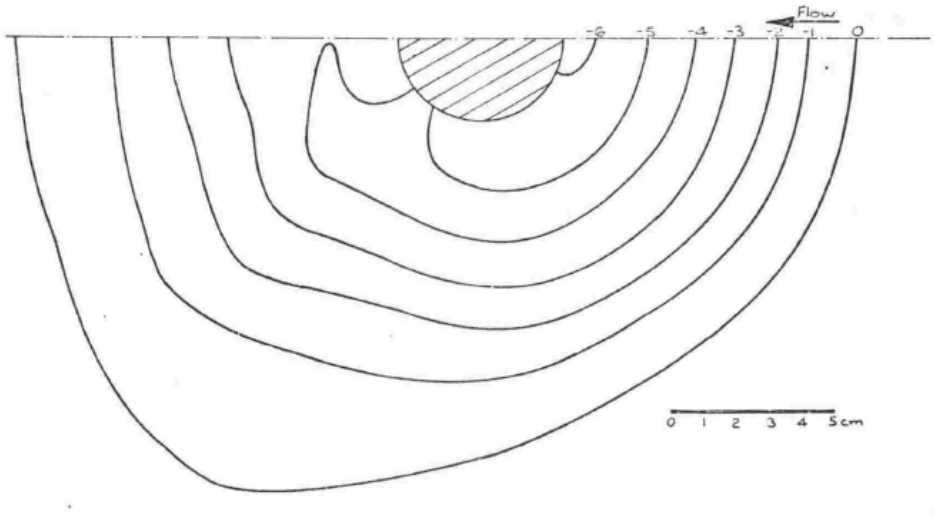

Figure 2.3 Contour plot of the resulting equilibrium scour hole after 2.5 hrs flow time (Melville 1975, p. 94).

2.3.2 Scour mitigation trials

Chiew (1992) reviewed existing methods of scour protection and trialled two new geometric shapes as countermeasures. The new measures were a vertical slot through a cylindrical pier, and a horizontal collar plate around the base of the pier.

The theory of the slot is to minimise or prevent down flow at the front of the pier by allowing the velocity profile pressure build-up to pass through the pier. Slots proportional to pier diameter (*d*) of *d*/2 width near the surface, and *d*/4 width near the bed were trialled in a flume tank.

Results are given as a percentage reduction of equilibrium scour depth as compared to a cylindrical control pier. It is suggested a slot near the surface effectively reduces water depth, and reduces scour by up to 30%. A slot near the bed reduces scour by up to 20%, but when combined with a collar can reduce it by 100% in clear-water conditions.

It is noted that bed shear velocity was kept at 0.9 times critical entrainment velocity, and that tests typically took 72 hrs to reach equilibrium. There is also a suggestion slots could be blocked by debris, thereby reducing performance.

Kumar et al. (1999) trialled slots of d/4 width in cylindrical piers under clear-water conditions. The aim was to study length of slots and flow approach angle. Slot lengths were full depth of water, and full depth plus anticipated equilibrium scour-hole depth (i.e. below normal bed surface). Three grades of sand were used; all fairly fine (0.78 mm < d_{50} < 1.54 mm). Critical shear velocity ratio was kept below one (u_*/u_{*c} between 0.75 and 0.98). Results indicate a slot extending down below the bed surface is more effective, however increased flow approach angles quickly negate the benefit of any slot.

Moncada et al. (2009) trialled slots of different length, aligned with the flow. They concluded that the longer the slot length the shallower the scour hole. Slots extending up from the bed were more effective than those extending down from the water surface. A slot of full water depth was most effective.

2.3.3 USQ projects

In recent years a number of related USQ engineering research student projects have been undertaken to study the effect of bridge piers on flow velocity, vortices, and scouring. These have generally been restricted to flume tank experiments.
Figure 2.4 shows a typical flume tank setup. Collectively these experiments demonstrate a development of alternative geometrically shaped piers.

One of the most advanced shapes tested was an aerofoil styled cross section (Drysdale 2008). The wake vortices and velocity profile were studied but the horseshoe vortex and sediment transport were not. Dimensions of the pier models were scaled down from those of a real bridge using the Froude scaling method.

Christensen (2009) further refined the aerofoil cross section, by adding a vertical slot through its long central axis. The horseshoe vortex, velocity profile and sediment transport were studied. The slot was reported to reduce scouring when compared with a benchmark cylindrical pier.

Figure 2.4 An example of a typical flume tank setup for a physical model experiment (Christensen 2009).

2.4 Empirical scour prediction formulas

Many researchers have developed pier scour prediction formulas from the results of experimental laboratory tests using scaled models in a flume tank (FDOT 2005). Most predict the maximum (equilibrium) scour depth. Formulas tend to correlate well with experimental results, but may not necessarily correlate well with larger scale real structures. There is limited field data available for validation with real large scale structures. The Sheppard equation has, however, been tested in some very large flume tanks, which are perhaps at the lower end of real scale structures.

Melville and Chiew (1999) also developed a formula for predicting the time required to achieve the equilibrium condition. The equilibrium condition is when the maximum scour hole depth is achieved and remains constant because the rate of incoming sediment transport equals the rate of outgoing sediment transport.

Zevenbergen (2005) compares results from three often cited scour prediction formulas. The three formulas nominated are:

- HEC-18 equation,
- Sheppard equation, and
- Melville equation.

Results tend to vary between the three equations. The Melville equation generally predicts the greatest scour (Zevenbergen 2005), while the Sheppard equation generally predicts the least scour.

2.4.1 HEC-18 equation

HEC-18 has been revised to a Fifth Edition (Arneson et al. 2012). The following equation and definition diagram (Figure 2.5) are from chapter 7 of the fifth edition. Pages 7.3 to 7.5 of the HEC-18 document should be consulted when using the equation in order to determine the appropriate correction factor values.

$$\frac{y_s}{y_1} = 2.0\, K_1 K_2 K_3 \left(\frac{a}{y_1}\right)^{0.65} Fr_1^{0.43}\,, \qquad (2.6)$$

where:

y_s = Scour depth, (m),

y_1 = Flow depth directly upstream of the pier, (m),

K_1 = Correction factor for pier nose shape,

K_2 = Correction factor for angle of attack of flow,

K_3 = Correction factor for bed condition,

a = Pier width, (m),

Fr_1 = Froude number directly upstream of the pier = $V_1 / (gy_1)^{0.5}$,

V_1 = Mean velocity of flow directly upstream of the pier, (m/s), and

g = Acceleration of gravity (9.81 m/s^2).

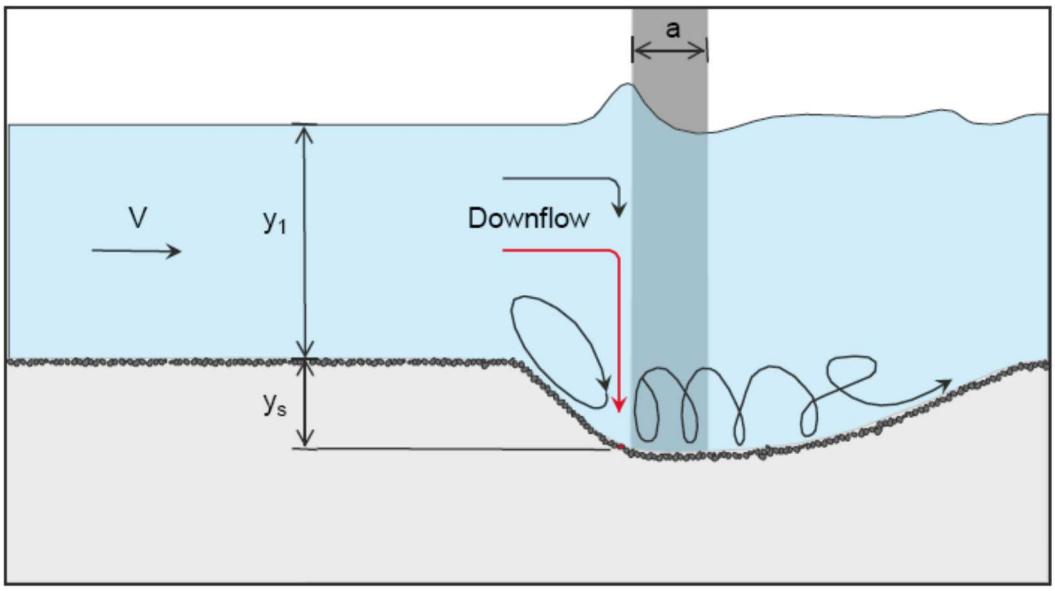

Figure 2.5 Definition diagram for the HEC-18 equation (Arneson et al. 2012).

2.4.2 Sheppard equation

The Sheppard equation is from the Florida Bridge Scour Manual (FDOT 2005). There are different equations for clear-water scour and for live-bed scour situations. The clear-water scour equation is applicable for flow velocity ratios of

$0.47 < V/V_c < 1.0$, where V_c must be calculated as specified in the manual. Pages 3.4, 3.7 and 3.10 of the manual should be consulted when using the equation in order to determine the appropriate parameters and calculation methods.

The Sheppard equation for clear-water scour is:

$$\frac{y_s}{D^*} = 2.5 \tanh\left[\left(\frac{y_0}{D^*}\right)^{0.4}\right]\left\{1 - 1.75\left[\ln\left(\frac{V}{V_c}\right)\right]^2\right\}\left[\frac{D^*/D_{50}}{0.4\left(D^*/D_{50}\right)^{1.2} + 10.6\left(D^*/D_{50}\right)^{-0.13}}\right] \tag{2.7}$$

where:

y_s = Maximum (equilibrium) scour depth,

y_0 = Flow depth directly upstream of the pier,

D^* = Effective diameter of pier,

D_{50} = Median diameter of sediment particles,

V = Depth-averaged velocity of flow upstream of the pier, and

V_c = Critical depth-averaged velocity (for sediment motion on a flat bed).

2.4.3 Melville equation

The Melville equation (Melville & Sutherland 1988, eq. 7) is:

$$\frac{d_s}{D} = K_I K_y K_d K_\sigma K_s K_\alpha \ , \tag{2.8}$$

where:

d_s = Maximum (equilibrium) scour depth,

D = Pier width (or diameter) normal to flow,

K_I = Flow intensity,

K_y = Flow depth directly upstream of the pier,

K_d = Sediment size (diameter),

K_σ = Sediment gradation factor,

K_s = Pier shape factor, and

K_α = Pier alignment factor.

The cited journal paper should be consulted for instructions, when using the equation, in order to determine the appropriate correction factor values.

When applied to the physical model and parameter values used in this project the Melville equation gives a maximum scour depth estimation of 0.106 m. Appendix C contains the method and calculations used to determine this result.

2.5 Numerical modelling

Numerical methods and CFD modelling have been developed and applied to the scouring problem within the last few years, but they have generally been limited to a single phase fluid flow.

2.5.1 Tao

Tao (2013) reviews recent developments in one and two phase CFD scouring models. Some explanation of relevant concepts and theories is given. These include:

- Turbulence models including k-ε, k-ω, and Reynolds Stress Model (RSM). RSM is available in Fluent and considered to be most accurate (Tao 2013).
- Discretisation by finite difference (FDM), finite volume (FVM), and finite elements (FEM). Fluent uses FVM; FEM is not recommended for fluid dynamics.
- For two phase situations, Eulerian models better suit fluid flow, and Lagrangian models better suit particle flow. Eulerian-Eulerian is satisfactory, and Eulerian-Lagrangian is satisfactory, but Lagrangian-Lagrangian is too complex and computationally expensive (Tao 2013).
- Meshing; structured or non-structured.
- Boundary conditions

Tao et al. (2015) trialled five different pier shapes in a 3-D single phase CFD model using COMSOL software. Some points of interest are:

- The domain was set up in two sections: a long coarsely-meshed first section to establish turbulent flow conditions at the inlet of a finely meshed second section containing the pier.
- Constant velocity at inlet one.
- Zero pressure outlet at both outlets.
- Non-slip walls at bottom and both sides.
- Sliding wall at top water surface.
- Eight mesh boundary layers at the non-slip pier walls.
- ~70,000 mesh elements in section two.
- Results were well displayed as velocity streamlines, and shear stress contour diagrams.

2.5.2 Zhu and Liu

Zhu and Liu (2012) modelled cylindrical piers and compared results with the Melville (1975) experiment. The software used was not named, but from the diagrams shown in their paper it does not look like ANSYS Fluent. They used a single phase Reynolds-Averaged Navier-Stokes (RANS) CFD model of flow, with standard k-ε turbulence model, and mathematical sediment transport models. The scour hole was developed by incremental updates of boundary adaptive mesh, based on the sediment transport equations.

They comment that an inlet velocity profile was not available from the test scenario so the model was run without the pier until reaching a stable profile. That profile was then used as the simulation input profile.

A smooth non-slip (friction) surface was used on the pier, and a rough non-slip surface on the riverbed ($2.5d_{50}$). They found a symmetric condition had to be used on the water surface to prevent unintended pressure loss. They advise it was a necessary simplification, although it is not correct as the water surface should be a free surface.

A number of simplifications were used to reduce computational load:

- Considerably shorter model space length; seven pier diameters before and ten diameters after the pier.
- Domain discretised with hexahedral blocks of non-uniform size; finer mesh in areas of greatest interest around the pier.
- Symmetric wall functions to avoid unnecessary fine meshing.

Results were similar to experimental results, but had a slight difference to the location and shape of the scour hole. They suggest this is because the model does not accurately allow for collapse of the scour hole due to gravity and the angle of repose of the bedding material. This suggests a two phase model should be better.

2.5.3 Xiong et al.

Xiong et al. (2016) modelled cylindrical piers and also compared results with the Melville (1975) experiment. By using an Eulerian two phase model they expected to produce a more reliable scour simulation. Software used was ANSYS Fluent but it appears to have been modified in some way by the “redevelopment function”. The paper mostly explains the methodology and theory behind their method. It does not provide much explanation from a practical modelling point of view, such as the parameter settings used.

Some comments of interest (Xiong et al. 2016) include:

- Each phase has a separate and independent volume fraction and velocity field.
- Solution is based on mass, momentum, and energy conservation equations.
- The model space is 20 pier diameters long (6 ahead / 14 behind).
- Mesh is based on a scour influence region; a square of side five diameters.
- Inflow for each phase was a pre-set pattern.

To reduce computation time the simulation was only run for 30 minutes, in the knowledge this would produce about 67% of full scour development (Xiong et al.

2016). Full scour development was expected to take about 2.5 hours, so equilibrium scour depth was not achieved. Results at the 30 minute run time were compared with the Melville experiment and considered to be fairly similar, although not identical. Results for a single phase model at 30 minutes run time were also compared; there are no details/description at all for the single phase model. It was concluded results for the two phase model were more accurate than the single phase model. This was taken as proof and justification of a two phase model being “more reliable”.

2.5.4 Knipe

Knipe (2014) used ANSYS Fluent, for a different purpose, in a USQ research project. Floodwater backflow behind a bridge was modelled using a water phase with an air phase above. Discrete analysis components were used in ANSYS workbench rather than complete analysis systems. This was to provide greater flexibility in how ANSYS can be used.

Various parameters associated with meshing and solution setup are mentioned Knipe (2014). Some specific choices are given; however the options are generally trialled to try and achieve the most reasonable results. A body sizing function is used to specify mesh size for specific chosen bodies, differently from other bodies.

2.6 Conclusions of review

Sediment particle characteristics and water flow velocity are the most significant factors in sediment transport. Accelerated water flow, when water is forced to go around an obstruction, is the most significant cause of local scouring.

A number of different pier cross sections have been trialled in an effort to reduce scouring around them, however they all still scour to some degree when used alone without any other countermeasure. There is scope for further research on slotted piers.

Previous research suggests slotted piers could be prone to debris blockage (Chiew 1992), and loss of performance at oblique approach angles (Kumar et al. 1999).

Most previous numerical modelling focuses on the modelling methods rather than the scouring results. However they usually include a comparison with existing experimental results in order to validate their model. Multiphase models are relatively new and there are very few which model scour around bridge piers.

Papers describing existing CFD models contain a number of suggestions which relate to reducing computational load, and may be suitable to implement in this project. They also provide some clues about appropriate parameter and variable choices.

Chapter 3

Methodology

Computer simulations are an efficient way to test bridge designs, when compared to using scale models in a flume tank. They offer a big advantage in that they can easily be altered to test the effect of changes to any of the input parameters. This project develops a computer simulation model to test bridge pier designs.

Computational Fluid Dynamics (CFD) was used to simulate multiphase flows around bridge piers. A commercial software package, ANSYS Fluent, was used.

An existing experimental pier scour trial, conducted with a physical scale model in a flume tank, was replicated as a two-phase CFD model using water and sand phases. This was done because experimental setup and results were available from the literature to validate correct operation of the simulation model. The validated model could then be used to test performance of a new and novel pier design.

The project was developed from a simple initial model and progressively expanded into the final model. Firstly, a 2-D steady-state model, in a horizontal plane, was used to examine the flow velocity around both a circular pier and the new pier design. Next a 2-D transient model, in a vertical plane, was used to examine a normal flow velocity profile and its interaction with a sand bed. Finally, a 3-D transient model was developed to examine flow disturbance and scouring around each of the piers.

3.1 Computer hardware and software

ANSYS Fluent CFD software (version 16.2) was used in this project because it is a well-known popular commercial product, and the USQ engineering faculty was already familiar with it. The USQ fully licenced version of software was not used because there was a problem in trying to setup remote access to the licence server

from the author's own computer. The student version (publically available from the ANSYS website) was used instead. The student version is a fully featured version but it has a maximum limit of 512k meshing elements/nodes available (ANSYS 2015). The meshing module can exceed this limit but the limit is enforced by the Fluent simulation module. Accordingly, the models were purposely kept within the meshing limit.

3.1.1 Hardware

The computer used for this project was a workstation class laptop. It was equipped with an Intel i7-6820HQ quad core processor, operating at 2.7 GHz, and eight gigabytes of memory. It was capable of performing the calculations but it was required to run for a very long time while doing so. Calculations could be done in blocks by using a specified number of time steps however these blocks were still typically a number of hours at a time, or overnight. There was a need to estimate how long a certain number of iterations may need to run, and calculations could not be stopped once a new block had commenced.

3.1.2 Software familiarisation and support

At project commencement the author had practically no prior experience with the ANSYS software. Familiarity was initially obtained from online tutorial type materials, and then further developed from experimental use of the program and reference to the user manuals.

The ANSYS software company no longer provide user or technical support to university students; they expect such assistance to be provided by the university. Consequently detailed ANSYS online tutorials which were available in the past are no longer available. The ANSYS website does provide some limited "self-service" assistance to students, this is in the form of fact sheets, basic usage tutorials, and links to some other external sources of tutorials.

The ANSYS software package contains on-board help files which include user manuals for each of the specialised modules within the package. The user manuals tend to give brief explanations and assume a certain amount of knowledge is already known, but they are quite helpful. The help files also contain a theory manual which explains some more complex aspects in greater detail.

Independently searching the internet also found some useful information available from various university websites. These include Cornell University, "*SimCafe CFD tutorials*" (Cornell 2015), and University of Connecticut, "*ANSYS tutorial 21, Using the Eulerian Multiphase Model for Granular Flow*" (ANSYS 2009).

When attempting to resolve the remote licencing problem, technical assistance was obtained from the USQ IT department and from LEAP Australia (agents for ANSYS in Australia), however they were not able to resolve the problem.

3.1.3 Workbench

The ANSYS software opens in "Workbench" which is a platform from which to open other more specific analysis modules. The other modules used were "Geometry", "Mesh", "Fluent", and "Results". These modules are available as an analysis system called "Fluid Flow (Fluent)" which groups all four modules together, however this project used the modules as separate entities and manually linked them together. This provided the opportunity to delete/change individual modules if required without losing information in the other modules. This technique was often used, especially with the Fluent module, as the easiest way to recover from having made an error or to ensure settings from a previous trial setup were not retained (Fluent did not always update all data for a new trial).

3.1.4 Geometry

The Geometry module is a 3-D computer aided drafting (CAD) program specifically tailored for ANSYS use. It is used to create the extent of the fluid

domain under analysis, and any physical features within the domain. The physical features include edges, surfaces, and bodies (fluid or solid). Externally created geometry can also be imported from other popular CAD programs.

The geometry required by this project was quite simple so it was drawn within the Geometry module itself, however using the Geometry module is different from using popular CAD software so a workable level of familiarity had to be developed.

The flume geometry was modelled as a full size replica of the physical experimental setup in order to try and reproduce realistic simulation results. The geometry was modelled in several stages with flow passing from one stage to the next through interior interfaces. The separate component parts were all grouped together as a single part, for meshing, so the mesh on each side of the interfaces was perfectly aligned for flow to pass seamlessly through them. The separate component parts allowed flexibility in how the components were utilised. At times some components were suppressed (hidden) in order to minimise mesh cell numbers in use, and computational load required. Figure 3.1 shows a close-up view of the domain in the vicinity of the cylindrical pier.

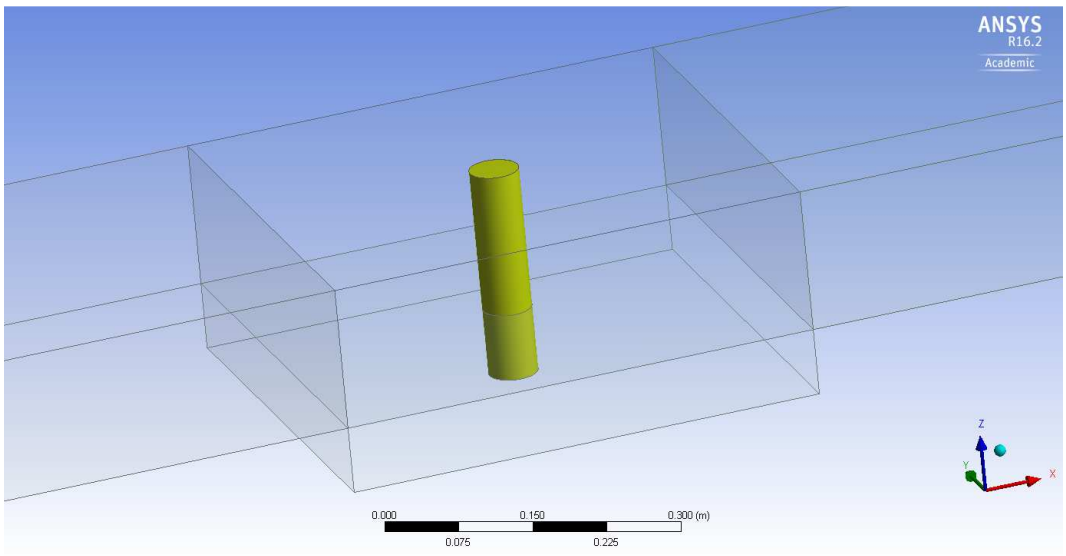

Figure 3.1 Close-up view of the model domain in the vicinity of the cylindrical pier.

The model domain was generally set out the same as the original physical experiment. A Cartesian co-ordinate system (x, y, z) was used, with the origin located at the intersection of sand surface level and pier central vertical axis. Water flow was in the positive x direction. The water inlet was located upstream (at x = -15 m) to allow fully turbulent flow to develop before reaching the pier. The water outlet was located downstream (at x = 4 m) to allow any dislodged sand to settle, and to allow for any pressure backflow effects upstream of the outlet.

The height of the water body was limited to z = 0.15 m deep, the same as water depth in the physical experiment; no provision was made for an air body above the water surface. Lack of an air interface could lead to a slight error because it does not allow any water surface upwelling to occur in front of the pier. The sand body was limited in both length and depth to reduce the number of mesh cells required. Initially length was 0.25 m upstream and downstream of the pier but this was extended to 0.75 m in some later simulations. Depth was z = -0.070 m, which is slightly deeper than scouring experienced in the physical experiment. The sand body is considerably shorter than the water body; therefore the floor of the water body is a false floor, with a surface roughness equal to sand grain diameter, wherever there is no sand body below it.

3.1.5 Mesh

Mesh is a program for meshing the domain of complex fluid and solid geometries. It contains various methods of creating and refining 2-D or 3-D meshes. It can display, check quality and report statistics about the mesh. For convenience it can also attach user friendly names to particular parts of the geometry, such as walls or inlet/outlet etc. Naming specific parts of the geometry can be very helpful for identifying them within the Fluent and Results modules.

The literature suggests fine meshing of a simulation model is required in order to produce accurate results, however this ideal may conflict with software and computer hardware limitations. The student version of ANSYS Fluent has a maximum limit of 512k nodes/cells, and the computer chosen for use also has some

limit to its maximum computing capacity. For these reasons the domain was minimised wherever possible in order to reduce the number of mesh elements required.

Ideally there should be fine meshing around the pier and the streambed surrounding it. Radiating out from these areas the mesh can progressively grow in element size; this was achieved by using a body sizing function based on the pier itself.

The pier is a solid item and not part of the fluid domain therefore it did not necessarily have to be meshed; at times it was represented as a void space in the fluid domain, with only its outer wall being represented. Meshing the pier was also beneficial at times, such as when there was a desire to alternate that portion of the domain between being fluid or solid (pier absent or present). It was also beneficial when the pier was required for display in the graphical result outputs.

The walls and floor of the flume were represented as non-slip surfaces in order to create friction drag along a boundary layer. In order to accurately simulate the boundary layer effect, edge or surface inflation was used to create finer meshing adjacent to these surfaces. The ceiling (and sometimes the walls) was represented as a symmetry wall. This was to ensure there was a slip surface with no boundary effect. The result was as if the boundary did not exist but the domain continued indefinitely, and it meant fine meshing was not required along the boundary.

Figure 3.2 shows a typical example of mesh on a vertical section of the sand and water bodies, through the pier axis.

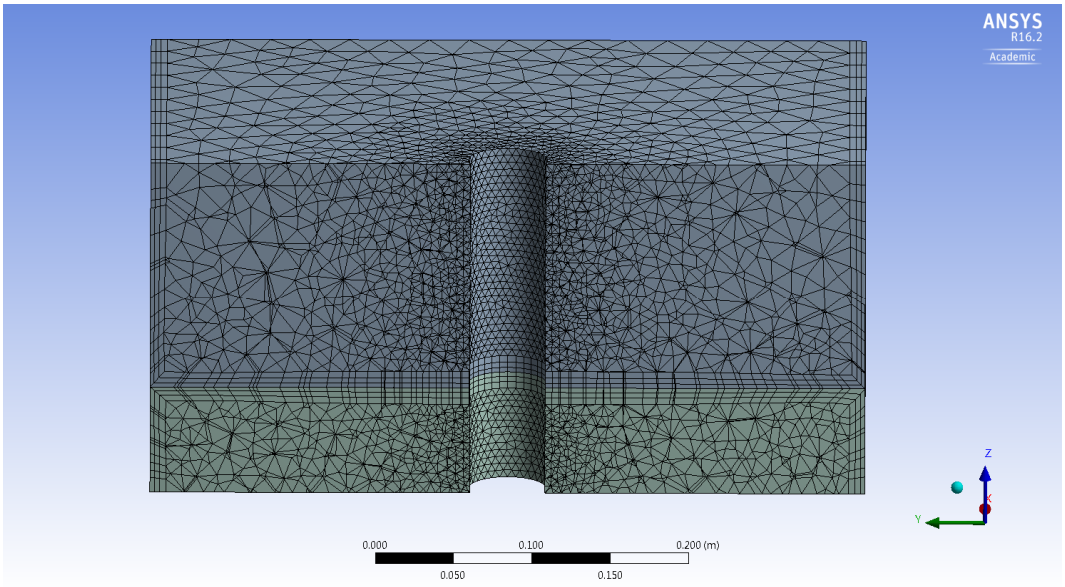

Figure 3.2 A section view of the sand and water bodies showing fine meshing in the vicinity of pier, walls and sand surface.

3.1.6 Fluent

Fluent is the analysis module which performs the simulation calculations. There are many sub-models, parameters, variables and options available in this module however only those relevant to this project are mentioned.

Within Fluent, some basic input values have to be specified but many parameters can be chosen from an inbuilt selection of sub-models. Many parameters for which past researchers have developed a functional relationship are available as sub-models; the most generally appropriate of these are often set as the default choice. There may be a choice of several sub-models, and there is usually additional user choices available. User choices include nominating a constant value or a user defined function (UDF).

Fluent contains three broad categories of operations: setup, solution and results.

Setup includes choice of a steady state or transient simulation, selection of turbulence and viscous models, specifying phase material properties and setting

boundary conditions. All simulations in this project used the standard *k*-ε turbulence model because it was expected to be satisfactory for the simple geometry and because it creates less computational load than other potentially more accurate turbulence models. All multiphase simulations in this project used the Eulerian multiphase model with dispersed phases because the Fluent user manual indicates the Eulerian multiphase model is the only multiphase model which can handle dense granular phases (ANSYS 2015a).

Solution includes specifying time step size for transient simulations, setting initial values for calculations, setting convergence limits for calculation accuracy and running the calculations.

Results allows for visual inspection of particular simulation result parameters displayed graphically on nominated surfaces in the domain. These results are available from within Fluent while it is running the simulation (however the simulation has to be stopped at the time). This is handy for periodically checking if the simulation is progressing as expected.

3.1.7 Results

The Results module, also known as “CFD Post”, is used to process result data after the simulation run has finished; this is referred to as post-processing. It has similarities with the results section in the Fluent module but it seems to be more user friendly, have a better graphics quality and be more flexible in how it can present outputs.

Simulation results can be difficult to interpret and may require close inspection of values on several surfaces. This is the case for examining velocity in specific parts of a 3-D domain because there are an infinite number of parallel planes either in front of or behind the plane currently on view. CFD Post results allow the user to create and name planes of particular interest at any specific location. Transparency of planes can also be adjusted so it is possible to see through a plane to another plane behind it. Determining the location of a sand surface from a volume fraction

display can also be difficult because the surface is not clearly defined and not located on a particular plane surface. An isosurface can be created to display an irregular surface at any locations where a specified value of a specified variable exists.

3.2 New pier design

A new pier cross-sectional geometry (Figure 3.3) is proposed, as a further development of shapes already tested by previous researchers. The aim of the new shape is to prevent, or at least minimise, acceleration of water flow as it is forced to divert around an obstruction such as a bridge pier. This would be achieved by purposely forcing water flow to pass through the centre of the pier rather than diverting around the outside of it.

The new shape is based on a slotted aerofoil section, but turned inside out. The two long outer sides are straight, so there should not be any acceleration of water flowing around the outside of them. Both the entry and exit of the slot are full width in order to present minimal obstruction to incoming water flow. The two inner surfaces of the slot are curves in order to smoothly streamline flow through the centre of the pier. For simplicity, the inner curved faces of a basic pier model are just a segment of a circle. Flow through the centre of the pier is accelerated to a high velocity, however the concrete pier should resist scouring internally.

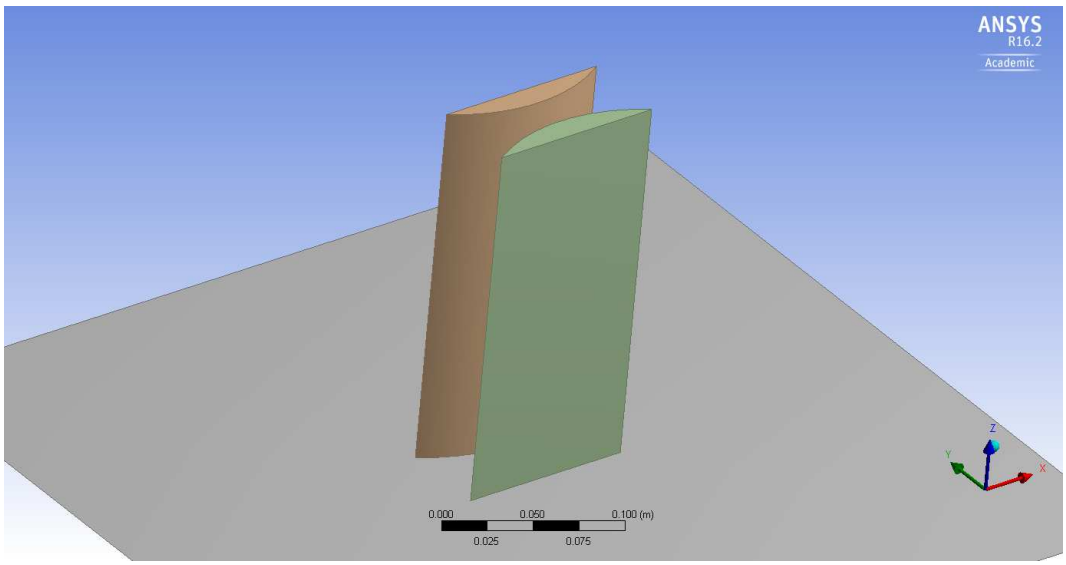

Figure 3.3 The new slotted pier design, aligned with stream flow direction.

The new pier used in the project has the same cross-sectional area as the cylindrical pier so that when used as a substitute it should provide the same compressive load bearing capacity. The overall width, normal to flow direction, is also the same as the cylindrical pier. This is in order to make a reasonable comparison of flow obstruction between the two pier designs. In order to have the same cross-sectional area, the new pier is longer in the flow direction however this is not expected to produce any adverse effects.

3.3 Experimental process

To develop a simulation model which replicates the original physical experiment an experimental approach was used. Parameter values and sub-model functions were selected in Fluent and trial simulation runs were conducted. Results were examined to see if they resembled the real situation.

Concepts and techniques from tutorials and previous research projects were used as a starting point. Initial parameter values were often left on default settings and then changed for subsequent runs, dependant on results obtained. Setting changes were generally confined to one parameter at a time so that any consequent change in

results could be observed. However the correct settings may require a combination of changes. Where possible informed judgement was used when changing settings, but at times a radical change was made to test how it would affect the outcome. The Fluent user manual was often consulted however it does not usually give explicit recommendations applicable to any particular situation.

Most existing tutorials and research projects were of only limited use as guidance because they had different objectives to this project. They usually expected or even intended for the granular sand phase to be moving relatively quickly in situations such as slurry transport, mixing tanks or sedimentation. In contrast this project requires the granular sand phase to generally remain stationary in the presence of flowing water, except for within the localised turbulent region around a pier. In this project, where sand movement is expected to occur it is expected to happen very slowly.

Simplified versions of the models were used at times to try and narrow down reasons for not achieving desired results. Keeping the situation as simple as possible reduced run times and made changes in results more obvious. The experimental process was difficult because trial runs take a long time before any results or change in results can be seen. Ideally, duration of trial runs should be for at least a full residence time to allow calculations to stabilise and produce meaningful results. Residence time is the time required for a particle entering the inlet to pass along the full length of domain and appear at the outlet.

While there was a desire to keep the model simpler, smaller and quicker, there was also a realisation that going too far with simplification could adversely affect the accuracy of results. It was observed that if mesh cells were made too large accuracy was reduced. It was also observed that if time steps were made too large, in order to speed up calculations, the simulation would become unstable and produce blatantly unrealistic results. In the worst cases the simulation would suffer a fatal and irrecoverable error.

To maintain stability of calculated results the Courant condition must be satisfied. The Courant condition is a relationship between mesh size and time step size such

that wave propagation (water flow velocity in this case) can not travel further than one mesh element in a single time step (Chadwick et al. 2004). Care must be taken when considering this because water velocity varies throughout parts of a turbulent simulation and the mesh size is quite small in parts of the domain.

When using a fine mesh in order to produce more accurate results it was necessary to also use small time steps, and that in turn created long run times. Therefore it took a very long time to see if a setting change was beneficial or not.

In 3-D models, trying to achieve realistic sand behaviour in the presence of flowing water was the biggest problem. There was a need to prove the model would work properly before it could be used on the new pier design.

3.4 Input data

3.4.1 Physical parameters

The physical input parameter values used are the same as for the Melville (1975) experiment described in section 2.3.1 of this dissertation. They are:

- Flume = 45.6cm wide x 44 cm deep x 19m long. 12.7cm false floor depth.
- Bed slope (S_0) = 0.0001.
- Flow depth (y_0) = 15cm.
- Inlet mean velocity (V_0) = 0.25 m/s.
- Discharge (Q) = 17.12L/s.
- Pier = 5.08cm diameter (1/9 width ratio).
- Sand: d_{50} = 0.385mm, ρ = 2.65, 32° angle of repose.

3.4.2 Normal flow conditions

Mean bed shear stress is calculated as:

$$\tau_0 = \rho g y_0 S_0 \quad (3.1)$$
$$= 1000 \times 9.81 \times 0.15 \times 0.0001$$
$$= \ 0.147 \ \ \text{kg m}^{-1}\ \text{s}^{-2}.$$

Friction velocity is calculated as:

$$u_* = \sqrt{\tau_0/\rho} = \sqrt{g y_0 S_0} \quad (3.2)$$
$$= \sqrt{9.81 \times 0.15 \times 0.0001}$$
$$= \ 0.0121 \ \ \text{m s}^{-1}.$$

The entrainment function is calculated as:

$$F_S = \frac{\tau_0}{(\rho_S - \rho) g d_{50}} \quad (3.3)$$
$$= \frac{0.147}{(2650-1000)\times 9.81 \times 0.000385}$$
$$= \ 0.0236 \ \ \text{(unitless)}.$$

The shear Reynolds number is calculated as:

$$Re_* = \frac{u_* d_{50}}{v} \quad (3.4)$$
$$= \frac{0.0121 \times 0.000385}{1.003 \times 10^{-6}}$$
$$= \ 4.656 \ \ \text{(unitless)}.$$

Referring to the Shields diagram, the F_s and Re_* values plot below the Shields function curve, therefore the sand will be stable under normal flow conditions.

The Shields diagram is indirectly used to determine the critical friction velocity, at the threshold of motion, for a given grain size. The Shields diagram requires values of entrainment function and shear Reynolds number as inputs, however formulas for both of these values also require the unknown critical friction velocity as an input. Solution requires an initial estimate followed by an iterative refinement process. The correct critical friction velocity solution is confirmed when co-ordinate values of entrainment function and shear Reynolds number plot exactly on the Shields function line.

Melville & Sutherland (1988) suggest an alternative estimation method whereby a chart of critical friction velocity versus a range of grain sizes is derived from the Shields diagram. This requires reading pairs of entrainment value and shear Reynolds number from the Shields function and solving their respective formulas as simultaneous equations, for both grain diameter and critical shear velocity. Plotted results allow a close estimate of the critical shear velocity to be directly read from the chart for any grain size in the plotted range. The chart must be specifically prepared using densities and fluid viscosity particular to the given situation. Such a chart (Figure 3.4) has been prepared using values relevant to this research project. The chart shows critical shear velocity estimated as 0.015 m/s for a grain size of 0.385 mm.

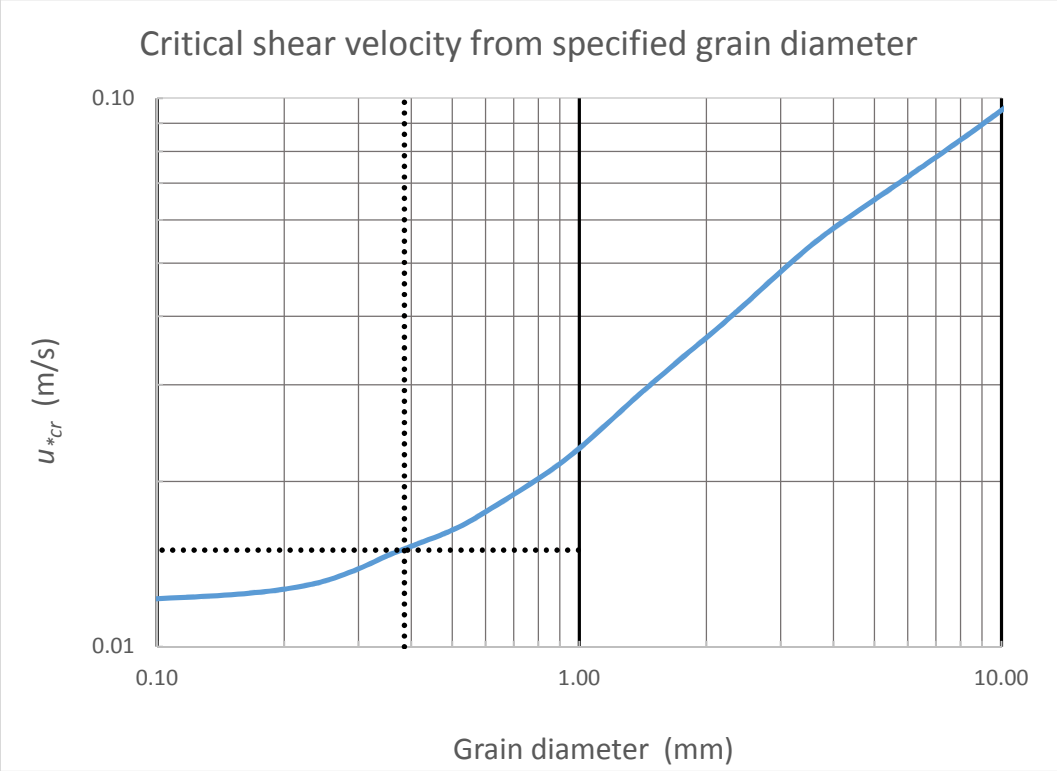

Figure 3.4 Chart prepared for estimation of critical shear velocity at threshold conditions; demonstrated for the 0.385 mm nominated grain size.

Melville & Sutherland (1988, eq. 2) indicate the critical shear velocity can be converted to a critical mean stream flow velocity (U_c) using the formula:

$$U_c = u_{*c} \times 5.75 \log\left(5.53 \frac{y_0}{d_{50}}\right) \qquad (3.5)$$

$$= 0.015 \times 5.75 \log\left(5.53 \frac{0.15}{0.000385}\right)$$

$$= \ 0.288 \ \ \text{m s}^{-1}.$$

Estimates of both critical shear velocity and critical mean stream velocity are both higher than actual values present in the normal flow of this model situation. This also confirms the given grain size will be stable under normal flow conditions.

3.5 2-D steady-state model

A 2-D steady-state single-phase model, in a horizontal plane, was created first because it was a fairly simple form of model to begin with. It was used to examine and compare velocity profiles and pressure distributions for the empty domain space, the model domain with cylindrical control pier, and the model domain with the new pier geometry. Neither the limit on cell mesh numbers, or computational runtime, were a problem in these 2-D models.

The first stage, of 14.75m length, was moderately meshed for development of turbulent inflow. The second stage, of 0.5m length, was finely meshed to study interactions around piers. The third stage, of 3.75m length, was moderately meshed to allow for turbulent outflow. All stages used edge inflation to provide finer meshing along the flume walls in order to accurately simulate boundary effects.

3.5.1 Empty domain space

The full flume length was modelled to allow realistic turbulent flow development, and to determine the velocity profile due to boundary effects. Smooth (zero roughness height) standard no slip walls were used. Convergence residual monitors were set at 1E-6. Initialisation was at water x-velocity of 0.25 m/s.

A contour plot of velocity profile (Figure 3.5) shows a friction boundary layer at the tank walls. Frictional drag slows the boundary layer down to zero velocity at the wall surface. Due to mass conservation, velocity in the centre of the flume is slightly accelerated beyond the nominal input velocity, so a velocity profile exists across the tank width. The plot suggests at least 10 m flume lengths are required for development of a stable velocity profile. A velocity profile was recorded at 14.75 m distance from the inlet so it could be used as an inlet velocity profile in subsequent shorter model domains. A maximum velocity of 0.283 m/s was observed.

Repeating the simulation with symmetry walls shows no frictional boundary layer is formed so the water velocity always remains consistent across the tank width.

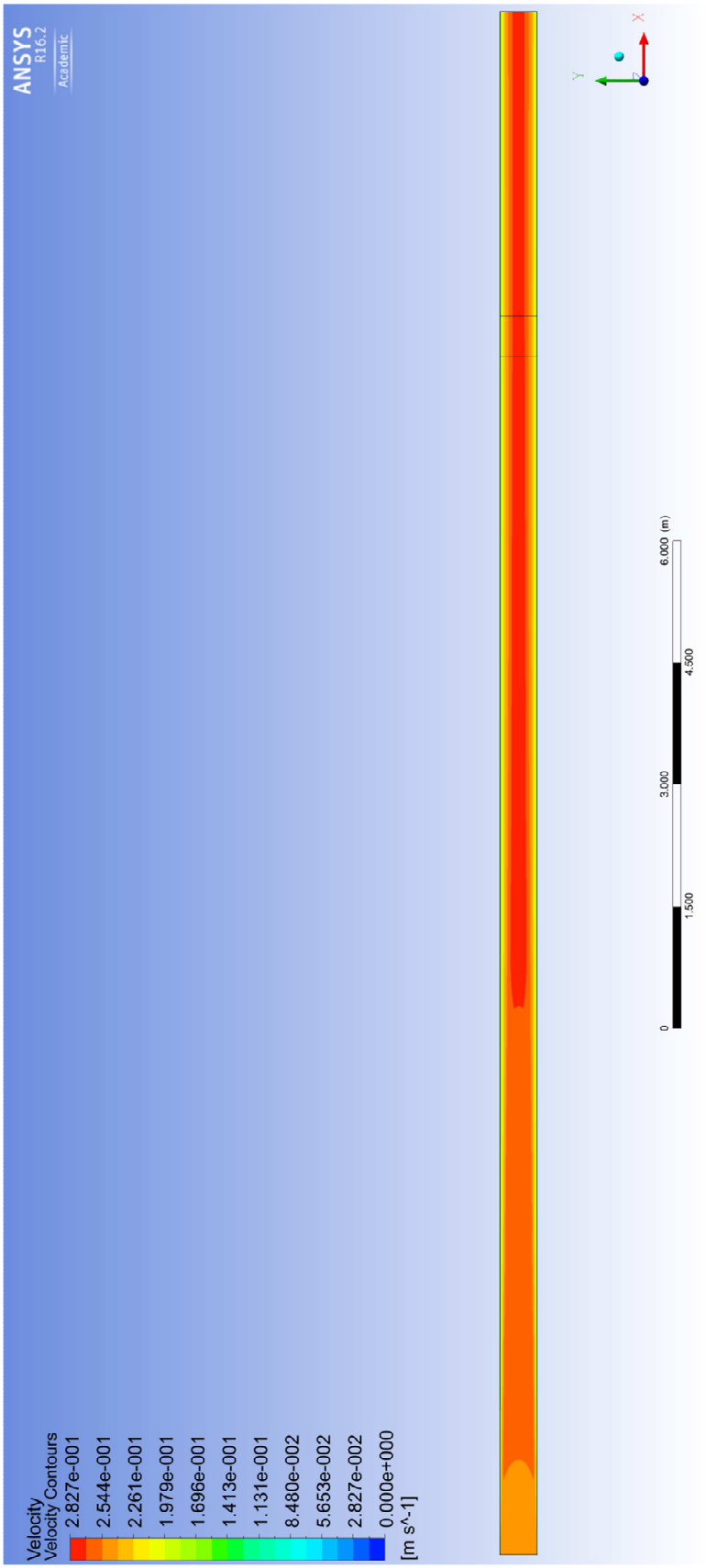

Figure 3.5 Water velocity profile in a horizontal plane across the width of the flume, when free of any flow obstructions (water flow is from left to right).

3.5.2 Cylindrical pier

The cylindrical pier was modelled in a reduced flume length. The longer length of stage one was suppressed leaving only stages two and three. Smooth (zero roughness height) standard no slip walls were used. Convergence residual monitors were set at 1E-6. The velocity profile recorded from the empty flume was used as an inlet velocity profile at the start of stage two. Initialisation used parameter values, from the inlet profile, present at the water inlet.

3.5.3 New pier design

The new slotted pier was modelled in a reduced flume length, similarly to the cylindrical pier. The velocity profile recorded from the empty flume was again used as the inlet velocity profile, and for initialisation.

3.6 2-D transient model

A 2-D transient model was created after initial attempts to run a 3-D transient model were found to be unsuccessful and were taking a very long time to run. The 2-D model is a vertical slice through the central longitudinal axis of a 3-D model. It is a multiphase model with water as the primary phase and sand as the secondary phase. As a 2-D model it used a lower number of mesh cells and could therefore run much faster and provide meaningful results much sooner.

The model was used to examine the effects of setting changes on sand movement. This was first done using a model without any flow obstruction; it only had a flowing water body above a sand body. In this situation the sand was expected to remain stationary.

Initial sand behaviour was found to be sensitive to initialisation conditions. Initialisation conditions are universally applied in all locations throughout the domain. Initial conditions of velocity or pressure which were suitable to the water

body were not suitable for the sand body. Unrealistic sand behaviour was evident in the results and the simulation was unable to recover from that situation.

The most appropriate initialisation technique was found to be using a temporary wall surface between the sand body and the water body, initialising the model with default values of zero pressure and velocity, and running it as a steady-state model until convergence of water flow was obtained. After convergence the temporary wall surface was changed back to an interior partition, sand was patched in to the sand body at a chosen volume fraction, and the model type changed to transient. The model was then run with very small time steps to minimise the shock reaction occurring at the interface between stationary sand and flowing water. After a few iterations the calculation residuals began to stabilise and time step size could be increased when calculation residuals were acceptable. This technique was used for all subsequent transient models.

The vertical 2-D model was also used with a water flow obstruction to examine sand movement due to the disturbed water flow. A vertical pier could not be used in the 2-D model as it would have completely blocked the water flow. Instead a circular section representing a pipe running perpendicular to the flow and just above the sand bed was used to divert flow toward the sand bed and cause scouring.

3.7 3-D transient model

The 3-D transient model is a multiphase model with water as the primary phase and sand as the secondary phase. It is used to examine the interaction between the sand and water phases. The model is required to run over an extended time period until local scouring around the pier reaches a maximum equilibrium depth. Initially this is an unknown duration however, from the original physical experiment, it was expected to be approximately 2.5 hours flow time.

For the 3-D model mesh cell numbers and simulation run times were significant factors. There was a need to keep the model domain fairly short in order to keep the total number of mesh cells within the 512k limit whilst providing the finest possible

meshing to accurately capture sand movement. The higher number of mesh cells required by the 3-D model significantly increased the calculation run times.

Several different domain lengths were trialled in order to seek a satisfactory compromise between adequate meshing and shorter calculation run times. A pre-recorded inlet velocity profile was used in all cases to compensate for the lack of turbulence development length at the inlet. A very short domain of only 0.5 m length, and moderately meshed, was found to be unsatisfactory. It achieved shorter run times but the mesh was too coarse to accurately simulate and display sand movement. The sand surface location was unclear because the mesh was too course to accurately define it.

A better alternative domain had a 1.5 m sand body and 2.0 m waterbody. It used body sizing functions to achieve fine meshing around the pier and sand interface regions. Over 400k mesh cells were used and time steps had to be 0.0001 seconds or less. Attempts to further increase the number of mesh cells in use tended to promptly exceed the maximum limit available.

Within Fluent, definition of the secondary phase includes a number of options for sand properties and interaction with the water phase.

Available sand properties include:

- Grain diameter;
- Granular viscosity;
- Granular bulk viscosity;
- Frictional viscosity;
- Granular temperature;
- Solids pressure;
- Radial distribution;
- Elasticity modulus; and
- Packing limit.

Available phase interactions include:

- Virtual mass;

- Drag;
- Lift;
- Turbulent dispersion;
- Turbulent interaction;
- Collisions;
- Mass transfer;
- Surface tension; and
- Interfacial area.

Not all of these options are applicable in all situations. Most are automatically set on the default choice to begin with and this is often a sub model. Some of these options have been varied in different trial runs. Sand viscosity settings and packing limit were varied; the drag interaction was also varied.

Calculation residual monitors were reduced to a less stringent setting of 1E-3 so that convergence of calculations could be achieved in less iterations and therefore speed up the overall process.

Runtime for the 3-D model meshed with 440k mesh cells was about one hour per 1000 time steps, when calculations converged within a couple of iterations. Maximum number of iterations was set at 20, but if 20 iterations were required for each time step runtime was considerably longer. With a fixed time step size of 1E-5 seconds, 1000 time steps was only one hundredth of a second flow time; therefore simulation runs took a very long time to produce any noticeable change in results. Even with a short domain, at this time step size simulations did not run for a full residence time; they usually only ran for less than one second.

When the same simulations were meshed more coarsely a larger time step could be used. Adaptive time stepping was also used in an effort to speed up the simulation. Adaptive time stepping is a feature in which the time step size is able to automatically vary up or down depending on the value of calculation residuals achieved. Using this technique it was possible to run simulations of 120 seconds flow time, however their accuracy was compromised and calculations sometimes became unstable so fixed time steps were generally used instead.

3.8 Sand flow model

A new and separate transient model was created in an effort to learn more about sand behaviour. The model had a sand secondary phase and an air primary phase so the primary phase would have negligible effect on the sand behaviour.

The model was a 3-D cube shaped domain with an internal horizontal wall surface part way up the internal volume space. Figure 3.6 shows the model in a 2-D diagram along the central vertical axis. Sand was patched in to the volume space above the internal wall and allowed to drain out, through a central hole, under gravitational force alone. There was no external inflow or outflow of either air or sand. There was a venting riser tube provided to equalise air pressure above and below the sand.

The purpose of this model was to examine the formation of a crater in the sand surface in the upper section, and the formation of a sand mound in the lower section.

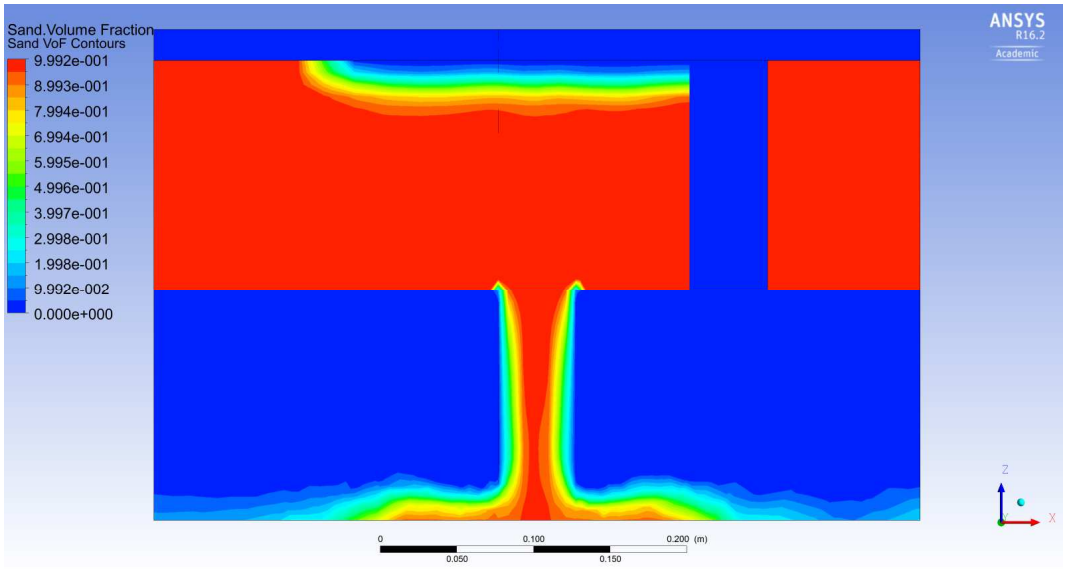

Figure 3.6 A model to examine sand behaviour as it drains freely under gravity alone.

Chapter 4

Results

4.1 2-D model in a horizontal plane

Velocity profiles surrounding the cylindrical control pier and the new slotted pier are noticeably different. The profile around the cylindrical pier has a small area of maximum velocity at each side, and is consistent with expectations based on previous research results. Figure 4.1 shows the resulting velocity profile surrounding the pier as water flows from left to right in the diagram.

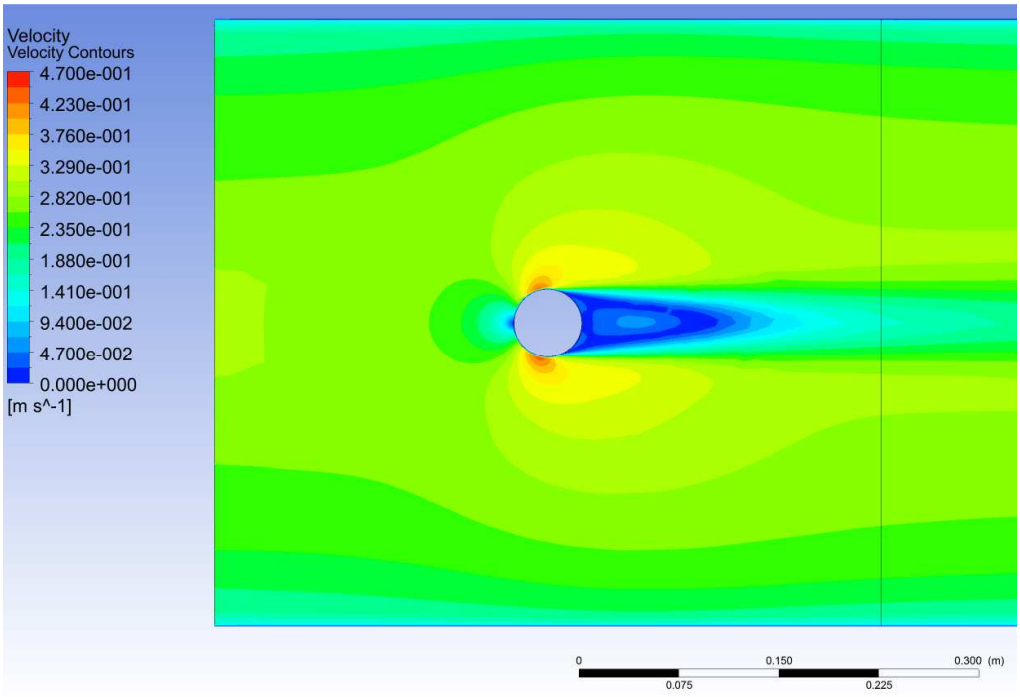

Figure 4.1 Water velocity profile due to flow obstruction from the cylindrical control pier (water flow is from left to right).

For a mean inlet velocity of 0.25 m/s, a maximum velocity of 0.43 m/s occurs at the sides of the pier in the red shaded areas. A small area of very low velocity appears at the nose of the pier where flow is obstructed and diverted down the face of the pier. A large tail area of very low velocity appears in a negative pressure area behind

the pier. Figure D.2 contains a wider view diagram, of this result, showing the downstream velocity stabilising as it travels toward the outlet.

The profile around the new pier has a maximum velocity within the centre of the pier; the highest velocity around the outside is 0.7 m/s less than for the cylindrical pier. Figure 4.2 shows the resulting velocity profile surrounding the new pier as water flows from left to right in the diagram. The scale used is the same as that of Figure 4.1 for ease of comparison.

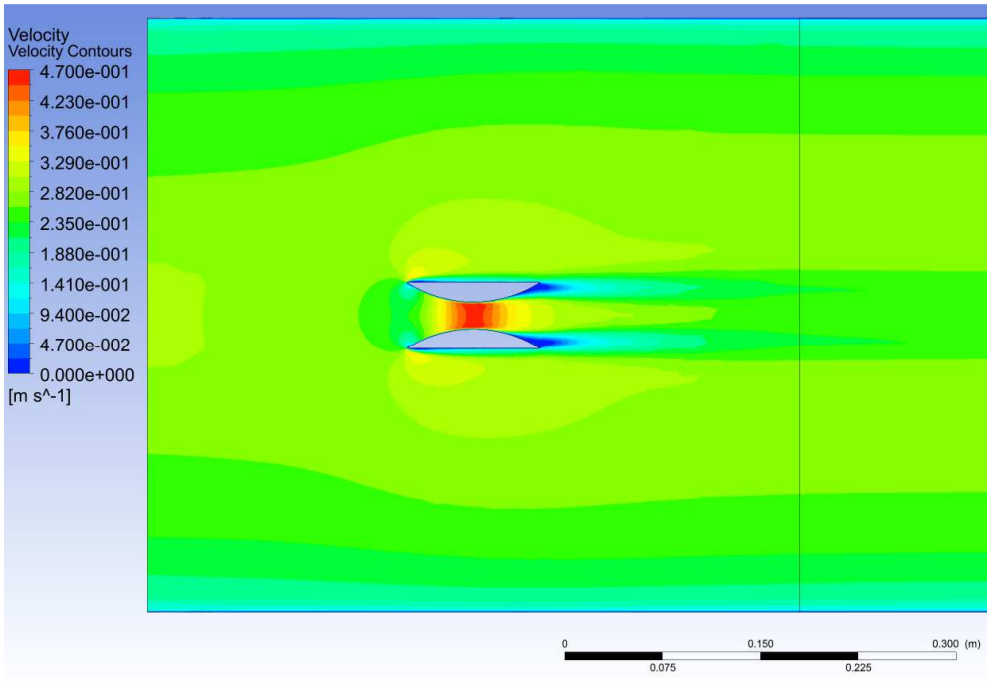

Figure 4.2 Water velocity profile due to flow obstruction from the new pier design (water flow is from left to right).

For a mean inlet velocity of 0.25 m/s, a maximum velocity of 0.47 m/s occurs in the slot at the centre of the pier. The highest velocity at the sides of the pier is approximately 0.36 m/s. Two small tail areas of very low velocity appear behind the pier sections. Figure D.3 contains a wider view diagram, of this result, showing the downstream velocity stabilising as it travels toward the outlet.

The results suggest the new pier design has potential to reduce scouring effects, compared to the cylindrical control pier, because of the reduced water velocity alongside the pier.

4.2 2-D model in a vertical plane

The 2-D vertical model was cost effective, in terms of run time, to experiment with parameter/setting changes.

In this model with no specific flow obstruction there should not have been any sand movement. The initialisation technique using a temporary lid over the sand body greatly improved sand behaviour, but the sand was still moving when it should have remained stationary.

A number of parameter variations were trialled in an effort to find out why sand behaviour was not realistic. Initial attempts included slower water velocity, increased sand density, and larger sand grain size. Basic theory suggests all of these measures should have slowed down or stopped sand movement however they did not appear to cause any noticeable difference.

Sand packing density was varied to control water movement within the sand body. Packing limits ranging between 0.63 and 1.0 were used. A packing density of 0.63 is the default value, based on an assumption of identically sized spherical sand grains. It allows for the maximum amount of void space between sand grains. In contrast a packing limit of 1.0 means there would not be any void space between sand particles, therefore there would not be any momentum transfer from water within the sand body. In this limiting case, momentum transfer from water to sand could only occur at the sand surface.

Further trials included selection of different drag and frictional viscosity laws. “Gidaspow” and “Syamlal-Obrien” drag laws were trialled, along with modified versions of each. The drag law was modified by factors smaller and greater than one. A factor of less than one was found to cause sand velocity to increase above that of water. A factor greatly larger than one (e.g. 1000) appears to slow sand velocity down. The Schaeffer frictional viscosity law was also trialled to see if it could increase frictional resistance between sand grains.

Figure 4.3 shows early results after a short flow time of 0.3 seconds. A contour plot of sand volume fraction appears to show sand scoured away from beneath the pipe. However after running the model for a longer period of 3.2 seconds (Figure 4.4), the sand appears to be levelling off along the whole sand bed length. Changes to the sand packing limit, viscosity properties and the phase interaction drag law did not overcome the problem but may have slowed the process down.

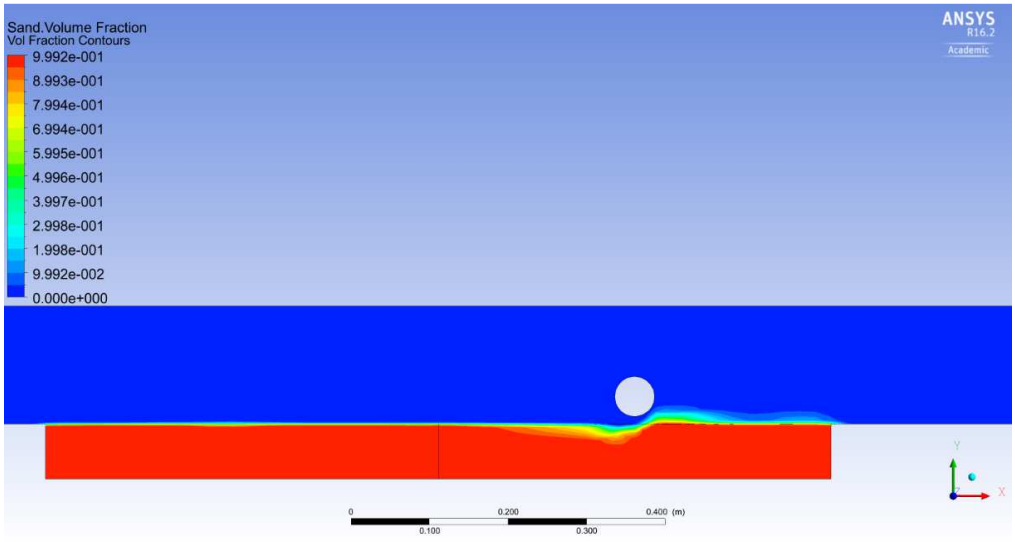

Figure 4.3 Early scouring results beneath a horizontal pipe after 0.3 seconds flow time in a 2-D vertical model (water flow is from left to right).

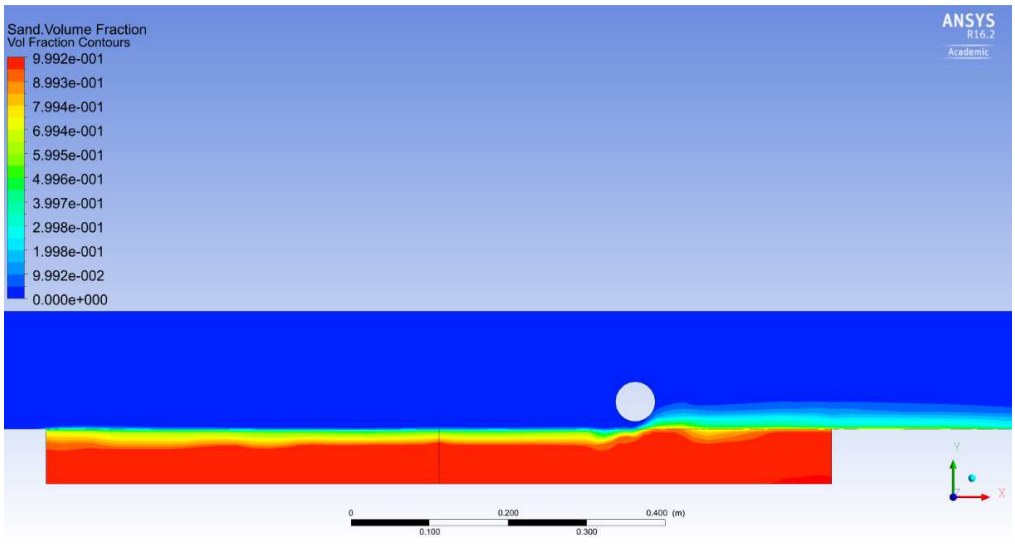

Figure 4.4 Sand bed scouring appears to level off after a longer flowtime of 3.2 seconds (water flow is from left to right).

4.3 3-D model

The model has been run in many forms including different domain lengths, different numbers of stages present, different meshing sizes and different time step sizes. In all cases so far the sand does not behave realistically. It moves too easily and quickly and appears to behave much more like a fluid than sand. It is likely something in the sand properties or phase interactions is not set correctly.

4.3.1 Early results

Early results from a model using initial sand at volume fraction 1.0 indicate that over a period of time sand appears to be scoured away from the whole general area rather than locally around the pier. Figure 4.5 shows an isosurface at 0.991 sand volume fraction. It appears to show most of the sand has been scoured away. However, at the same situation and point in time, Figure 4.6 shows an isosurface at 0.90 sand volume fraction; it appears to show most of the sand is still present. Appendix D shows some additional results, at different volume fractions, at the same point in time.

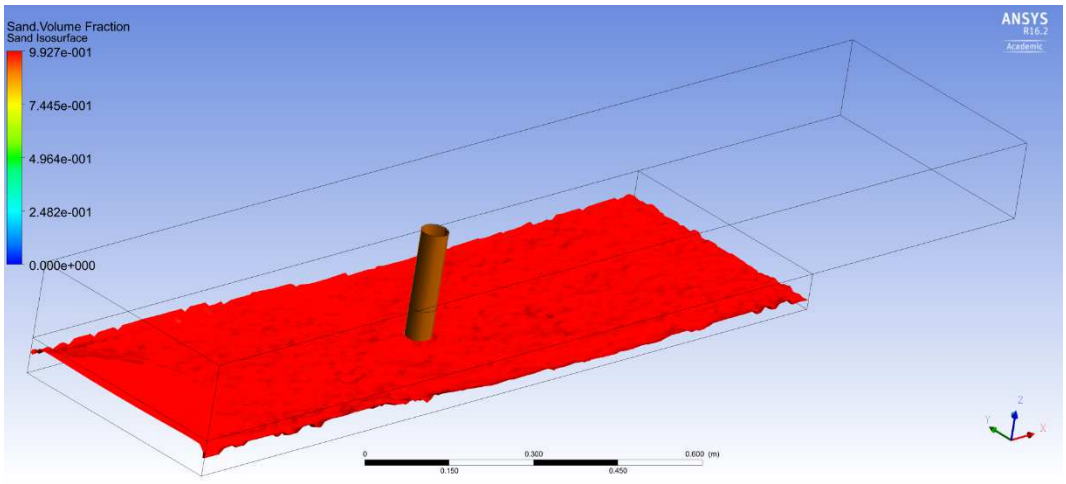

Figure 4.5 An isosurface at 0.991 sand volume fraction appears to show most of the sand has been scoured away.

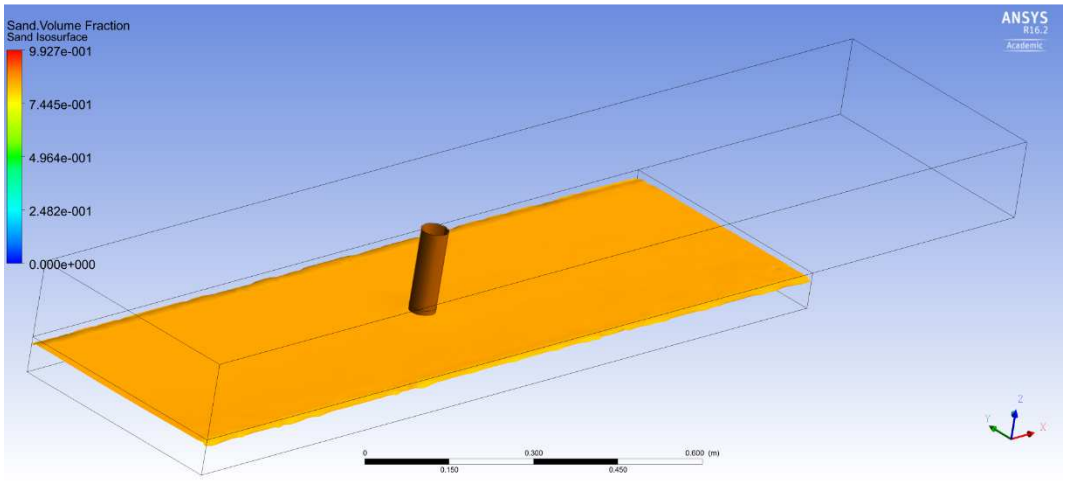

Figure 4.6 An isosurface at 0.90 sand volume fraction appears to show most of the sand is still present.

The presence or location of a sand surface requires some interpretation. As a bulk quantity, real sand either exists in a location or it does not. Sand at a volume fraction of less than one must be interpreted as a number of sand grains suspended in water, rather than a bulk quantity of sand. In practice (in the model) a sand volume fraction of one becomes non-existent as soon as the simulation begins to run, therefore a volume fraction of slightly less than one is the best available.

4.3.2 Improved results

Improved results were obtained from a model using finer meshing and a combination of parameter changes including the drag and friction laws. The model used smaller time steps and took around 70 hours runtime to produce 3.5 seconds simulated flow time. Initial sand volume fraction was at the default value of 0.63 in this model, and all subsequent models. Table 4.1 shows settings used in this model.

Table 4.1 Fluent settings used in the cylindrical pier model.

Mesh elements	429k
Time steps (Initial/Final)	1E-5 / 5E-4 seconds
Runtime	70 hrs, for 3.52 s flowtime
Sand Granular Viscosity	Syamlal-Obrien
Sand Granular Bulk Viscosity	Lun et al.
Sand Frictional Viscosity	Schaeffer
Sand Angle of repose	32 degrees
Sand Frictional packing limit	0.63
Sand General packing limit	0.63
Phase interaction, Drag function	Gidaspow, modified by 1000
Phase interaction, Lift function	Moraga

Figure 4.7 shows there is less generalised scouring, and some suggestion of localised scouring to either side and behind the pier. Location and shape of the scouring suggest it is a result of disturbance from the pier, however it is not consistent with realistic expectations.

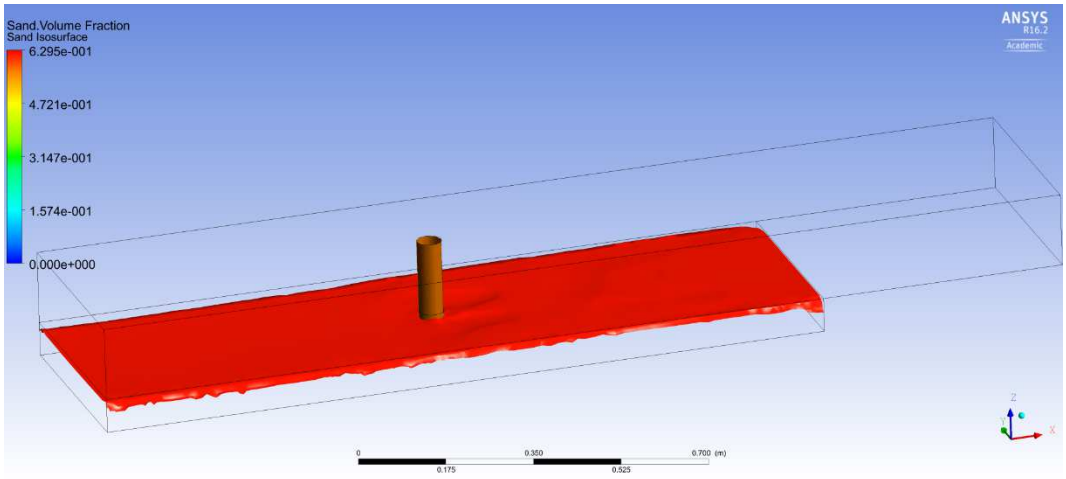

Figure 4.7 An isosurface at 0.62 sand volume fraction after 3.52 seconds flow time. It shows a suggestion of localised scouring to the sides and behind the pier, with very little generalised scouring.

After another 20 hours runtime, making a total of 90 hours, the improved model started showing signs of generalised scouring which wiped out any sign of localised scouring. Figure 4.8 shows the result after 12 seconds flow time. Sand was behaving more like a fluid and seeking a level surface over time, so the same problem still existed but was taking longer to manifest itself.

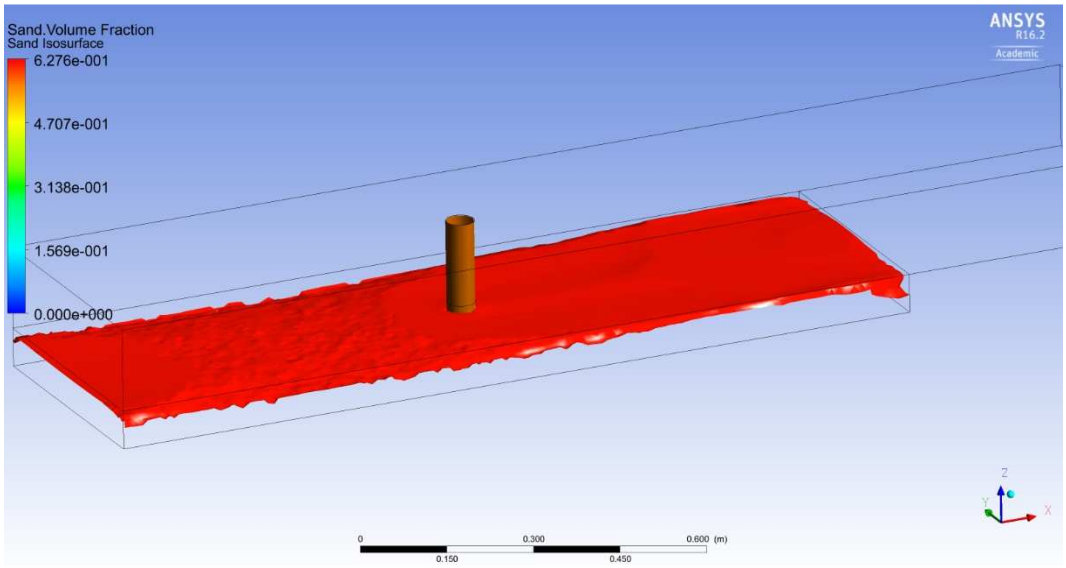

Figure 4.8 An isosurface at 0.62 sand volume fraction after 12.0 seconds flow time. Generalised scouring is very prominent just back from the inlet, and localised scouring adjacent to the pier has been wiped out.

After 20 seconds flow time, Figure 4.9 shows generalised scouring has occurred over the entire surface area. , An isosurface no longer exists at a volume fraction of 0.62 as used in the previous result diagrams, so this diagram is at 0.615 volume fraction.

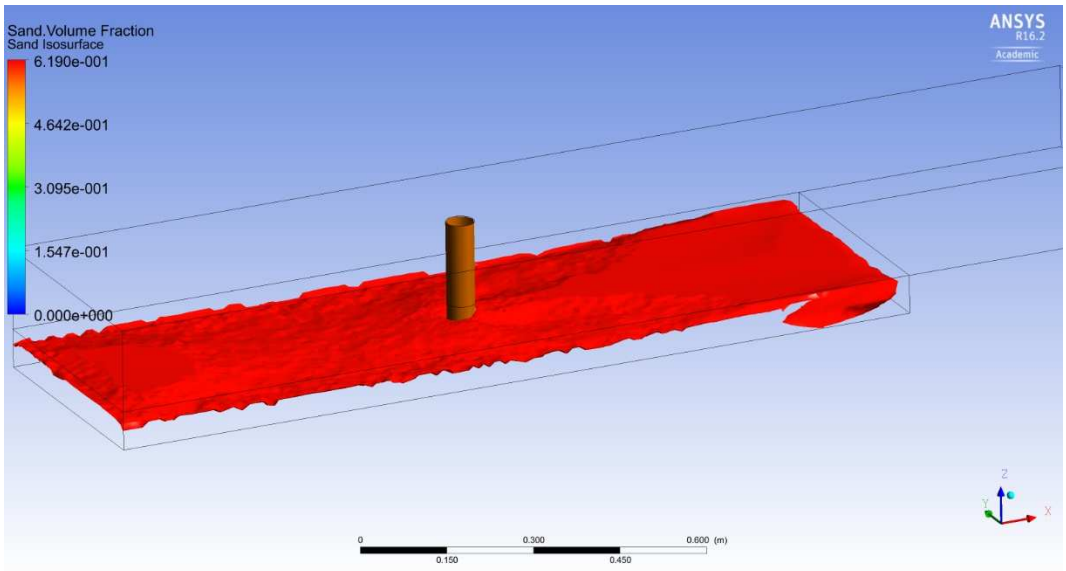

Figure 4.9 An isosurface at 0.615 sand volume fraction after 20.0 seconds flow time. Results are similar to those after 16.0 seconds but generalised scouring has removed some sand volume from the entire surface area.

Appendix D contains a series of result diagrams spanning 3.5 to 20.0 seconds flow time. They show a slow process of general scouring progressively getting worse.

Following this simulation run a decision was made to not make any further attempts at refining the model as time was running out. Any additional alterations to the model would need around 70 hours runtime to see if they were beneficial, and there appears to be something definitely wrong with settings related to sand movement. Remaining time was required for conclusions and report findings.

4.4 Sand behaviour model

The sand behaviour model was used to prove that both a sand crater surface and a sand mounded surface could be observed in the simulation results if they actually existed. Figure 4.10 shows the results of the sand behaviour model after 0.8 seconds of flow time. Expected localised scouring had not been seen in any of the simulation results so this visual confirmation gave a degree of confidence in the capability of the simulation model results to display localised scouring.

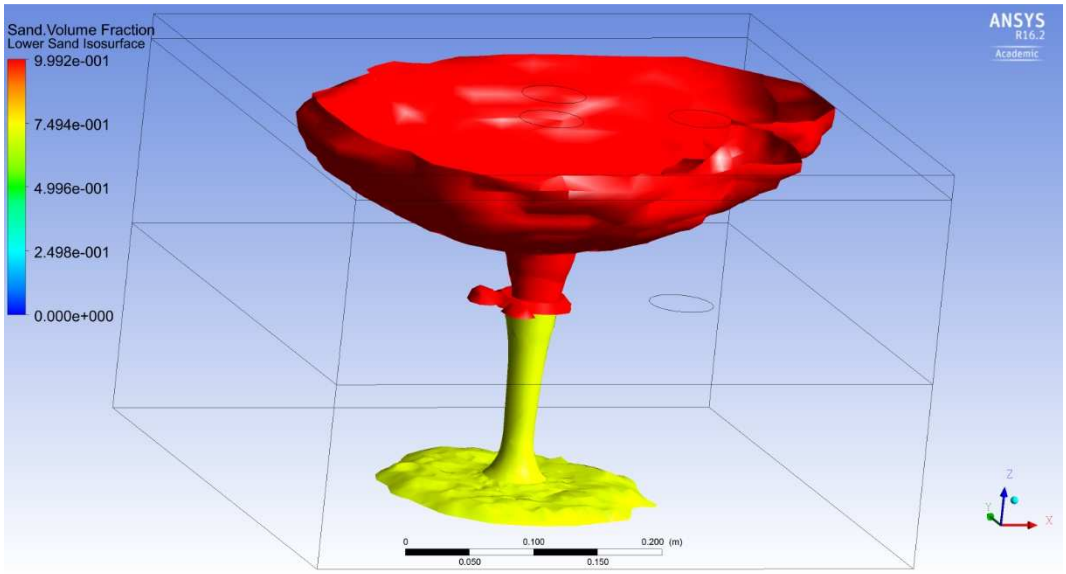

Figure 4.10 Visual proof that both a sand crater surface and a sand mounded surface can be seen in the results if they actually exist.

The crater surface is at a volume fraction of 0.9991 which is just marginally less than the maximum fraction present in the results. This is a high fraction because the sand was initially patched in at a volume fraction of 1.0 so it was firmly packed. The mounded sand in the lower section is at a volume fraction of 0.7 because it has simply fallen under the force of gravity and is therefore only loosely packed.

When the sand behaviour model had run for a longer period of 5.0 seconds flow time, both the upper and lower sand surfaces were attempting to level off as might be expected from liquid behaviour.

4.5 New pier design

A simulation trial was conducted using the new pier design. As the simulation model had not yet proven itself to be reliable, this was done purely as an experiment rather than a genuine test of pier performance. The new pier design is more streamlined than the cylindrical pier so there was a possibility of reduced water flow disturbance. Fluent settings used are listed in Table 4.2, and are essentially the same as used in the most recent cylindrical pier trials.

Table 4.2 Fluent settings used in the new pier model.

Mesh elements	440k
Time steps	50k @ 1E-5
Runtime	40 hrs, for 0.5 s flowtime
Sand Granular Viscosity	Syamlal-Obrien
Sand Granular Bulk Viscosity	Lun et al.
Sand Frictional Viscosity	Schaeffer
Sand Angle of repose	32 degrees
Sand Frictional packing limit	0.63
Sand General packing limit	0.63
Phase interaction, Drag function	Gidaspow, modified by 1000
Phase interaction, Lift function	Moraga

Initialisation and initial convergence of calculations proved to be difficult. Initial convergence of water flow calculations could not be achieved in a steady state, but was achieved in a transient state instead. After convergence and removal of the temporary initialisation sand lid, calculations progressed at very small time steps but were a little unstable. Stability appeared to recover however it was observed that the calculation residual for sand volume fraction was slowly increasing.

Figure 4.11 shows results after 0.5 seconds flow time. There is significant unrealistic gouging of sand from near the inlet but there does not appear to be much general scouring over the rest of the sand surface area. There is also a suggestion of localised scouring adjacent to and upstream of the pier. The location and shape of this scouring suggest it is due to flow disturbance from the pier however there is no benchmark to indicate what a scour pattern around this pier design should look like.

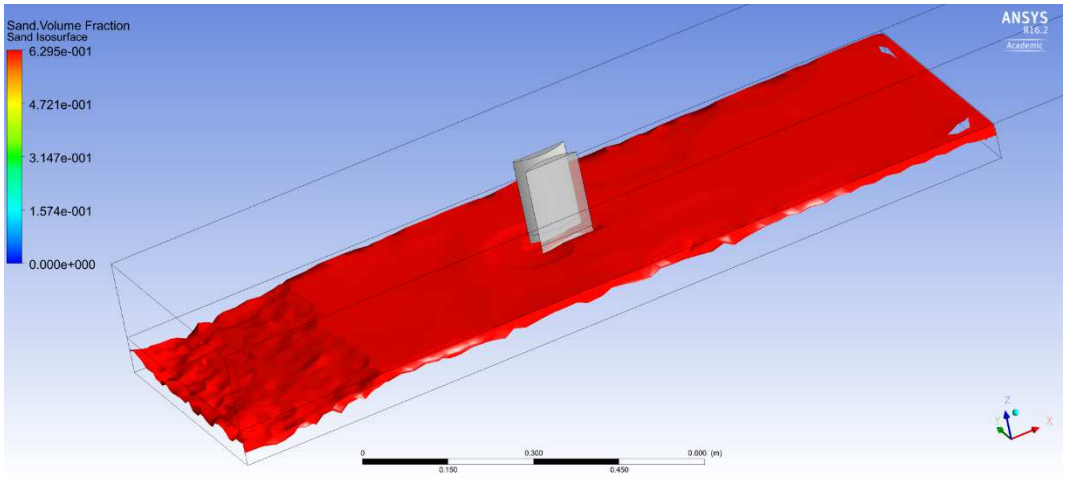

Figure 4.11 Initial simulation results for the new pier design appear to show unrealistic gouging and a suggestion of local scouring near the pier. These results are unverified and unreliable.

4.6 Empirical estimates

Three popular empirical estimation formulas have been used to estimate the maximum equilibrium scour for the original physical scouring experiment. The three formulas are:

- HEC-18 equation,
- Sheppard equation, and
- Melville equation.

The estimated results were intended to be compared with simulation results from the model however the model has not been able to produce any realistic results for comparison. Alternatively, Table 4.3 compares the estimated results with the original experiment and gives an indication of what might have been expected from the simulation model. Full Calculations from each formula are included in Appendix C.

Table 4.3 Result comparison for different scour estimation methods.

Estimation method	Equilibrium scour depth (mm)
Physical experiment	≈ 70
HEC-18 equation	82.8
Sheppard equation	104.9
Melville equation	105.8

These estimates differ slightly from the findings of Zevenbergen (2005) in that the HEC-18 equation gives a shallower scour than the Sheppard equation. The Melville equation is consistent in predicting the greatest scour however it is only slightly greater than the Sheppard equation.

Chapter 5

Potential future development

5.1 Further research

5.1.1 Current model

Successful simulations using the current model are dependent on achieving realistic sand behaviour, therefore there is a need for further study of sand behaviour. There is a need to develop specific models to objectively quantify sand movement relative to parameter/setting changes.

There could be benefit in creating a simple model of sand with an inclined surface at an angle of less than the angle of repose. The objective would be to find the correct combination of parameter settings to keep the sand stationary over an indefinite time period, rather than levelling out as liquid behaviour would do.

While this project requires no sediment transport to occur in a general sense, there may be benefit in researching a different model in which sand transport is intended to occur. This could perhaps provide more insight into the appropriate parameter and setting choices for a sand phase.

Further development of the current model could include:

- Use of a different turbulence model.
- Use of the Dense Discreet Particle (DDPM) model.
- Consideration of other Fluent parameter choices and values.

5.1.2 Model application

Further research areas could include:

- Cohesive and non-uniform soils
- Unsteady flow, rising to a peak then receding

5.1.3 New pier design

The new pier could be further developed by:

- Slightly concave outer walls.
- Streamlined spline shaped inner walls.
- Optimised proportions/dimensions.
- Exhaust outlet shaping, to influence the outlet jet.
- Holes from outer to inner walls, acting as venturis.
- Steel guide plates at the inlet, to improve streamlining of inflow.

Chapter 6

Conclusions

Both 2-D and 3-D simulation models have been created using the geometry and input parameters from a physical experiment. Simulations produced by the 3-D models are not accurate; sand behaviour in the presence of flowing water is not realistic. At present, testing of pier designs with the 3-D models can not be used for predicting potential scouring effects.

- Research of relevant background information has been conducted. Information on bridges, sediment transport, scouring and CFD modelling has been incorporated into this project.
- A 2-D single-phase steady-state model has been developed and used to examine the flow velocity profile around both a cylindrical control pier and a new slotted pier design.
- The initial model has been further developed into a 3-D two-phase transient model.
- The 3-D two-phase model does not function properly; sand movement is not realistic. Attempts to calibrate its performance by selecting appropriate Fluent parameters and values have not been successful.
- The 3-D two phase model is clearly not functioning correctly therefore it has not been validated against results from the physical experiment.
- Performance of the new pier design has been simulated in both the 2-D and 3-D models. The 2-D model indicates the pier design has potential to produce less scouring than a cylindrical pier. The 3-D model does not function accurately so results are not reliable.
- Modelling results have not been compared with estimates from empirical formulas because the modelling results are clearly unrealistic. Empirical formulas have been used to estimate the results which were to be expected from the model.

List of References

ANSYS 2009, *Tutorial 21. Using the Eulerian Multiphase Model for Granular Flow*, web document, ANSYS Inc., viewed 9 May 2016, <http://www.engr.uconn.edu/~barbertj/CFD%20Training/Fluent%2012/>.

ANSYS 2015, *ANSYS Student brochure*, pdf web document, viewed 25 November 2015, <www.ansys.com>.

ANSYS 2015a, *Fluent user manual*, ANSYS software package: on-board help files, ANSYS Inc.

Arneson, LA, Zevenbergen, LW, Lagasse, PF & Clopper, PE 2012, *Hydraulic engineering circular No. 18: Evaluating scour at bridges*, 5th edn, U.S. Department of Transportation, Federal Highway Administration.

Chadwick, A, Morfett, J & Borthwick, M 2004, *Hydraulics in civil and environmental engineering*, 4th edn, Spon press, Great Britain.

Chiew, YM 1992, 'Scour protection at bridge piers', *Journal of Hydraulic Engineering*, vol. 118, no. 9, pp. 1260-69.

Christensen, ZM 2009, *Reduction of Local Scour Around Bridge Piers: Combined System of Aerofoil and Slot*, University of Southern Queensland, Toowoomba.

Cornell 2015, *SimCafe CFD tutorials*, webpage, Cornell University, viewed 10 May 2016, <https://confluence.cornell.edu/display/SIMULATION/FLUENT+Learning+Modules>.

Drysdale, DM 2008, *The effectiveness of an aerofoil shaped pier in reducing downstream vortices and turbulence*, University of Southern Queensland, Toowoomba.

FDOT 2005, *Bridge scour manual*, Department of Transportation, Florida.

Fu, G 2013, *Bridge Design and Evaluation: LRFD and LRFR*, Wiley, Hoboken, New Jersey.

Harik, IE, Shaaban, AM, Gesund, H, Valli, GYS & Wang, ST 1990, 'United States Bridge Failures, 1951–1988', *Journal of Performance of Constructed Facilities*, vol. 4, no. 4, pp. 272-7.

Henderson, FM 1966, *Open channel flow*, McMillan, New York.

Kumar, V, Ranga Raju, KG & Vittal, N 1999, 'Reduction of local scour around bridge piers using slots and collars', *Journal of Hydraulic Engineering*, vol. 125, no. 12, pp. 1302-5.

Laursen, EM and Toch, A 1956, *Scour around bridge piers and abutments*, cited in Melville (1975).

Melville, BW 1975, Local scour at bridge sites, University of Auckland, Auckland.

Melville, BW & Chiew, YM 1999, 'Time scale for local scour at bridge piers', *Journal of Hydraulic Engineering*, vol. 125, no. 1, pp. 59-65.

Melville, BW & Sutherland, AJ 1988, 'Design method for local scour at bridge piers', *Journal of Hydraulic Engineering*, vol. 114, no. 10.

Moncada, AT, Aguirre, J, Bolivar, JC & Flores, EJ 2009, 'Scour protection of circular bridge piers with collars and slots', *Journal of Hydraulic Research*, vol. 47, no. 1, pp. 119-126.

Nalluri, C & Featherstone, RE 2001, *Civil engineering hydraulics*, 4th edn, Blackwell Science, Oxford.

Tao, J 2013, *Fusion of numerical modelling and innovative sensing to advance bridge scour research and practice*, PhD dissertation, Case Western Reserve University, Cleveland, Ohio.

Tao, J, Li, J & Yu, X 2015, 'Streamlining of Bridge Pier as a Scour Countermeasure: A Feasibility Study', *Journal of IFCEE 2015*, pp. 319-29.

Wardhana, K & Hadipriono, F 2003, 'Analysis of Recent Bridge Failures in the United States', *Journal of Performance of Constructed Facilities*, vol. 17, no. 3, pp. 144-50.

Zevenberger, LW 2005, *Comparison of the HEC-18, Melville and Sheppard Pier Scour Equations*, web document, viewed 25 March 2016, <http://scour-and-erosion.baw.de/conferences/pdf/icse5/Proceedings_5-ICSE-12_FHWA.pdf>.

Xiong, W, Tang, P, Kong, B & Cai, CS 2016, 'Reliable Bridge Scour Simulation Using Eulerian Two-Phase Flow Theory', *Journal of Computing in Civil Engineering*, January 2016, ASCE.

Zhu, Z & Liu, Z 2012, 'CFD prediction of local scour hole around bridge piers', *Journal of Central South University of Technology (English Edition)*, vol. 19, no. 1, pp. 273-281.

Appendix A

Project specification

ENG 4111/4112 Research Project

Project Specification

For:	Gary Nankervis
Title:	Computer simulation of scouring around bridge piers
Major:	Civil Engineering
Supervisor:	Dr Andrew Wandel
Sponsorship:	Faculty of Health, Engineering and Sciences
Enrolment:	ENG4111 – EXT S1, 2016 ENG4112 – EXT S2, 2016

Project Aim: To develop a 3D computational fluid dynamics (CFD) model for simulating water flow and river bed scouring around bridge piers. To critically examine an alternative bridge pier design, by use of the model.

Program: Issue A, 16th March 2016

1. Research background information (scouring, sediment transport, CFD modelling).
2. Develop a single phase steady state model to analyse flow velocities for a new and novel pier geometry.
3. Further develop the model into a two phase transient model.
4. Validate and/or calibrate the model against pre-existing experimental results by replicating all the parameters of a benchmark experiment involving circular piers.
5. Use the two phase model to test scouring around the new pier design.
6. Compare modelling results with traditional empirical formula based scour estimates for the benchmark circular piers.

As time and resources permit:

1. Trial and evaluate different geometric variations.
2. Trial and evaluate different flow approach angles.

Agreed:

Student Name:	Gary Nankervis	Supervisors Name:	Dr Andrew Wandel
Date:	16/3/2016	Date:	16/3/2016

Appendix B

Melville experiment results

B.1 Intermediate scour hole

B.2 Equilibrium scour hole

B.1 Intermediate scour hole

Figure B.1 shows a contour plot of the intermediate scour hole after 0.5 hrs flow time (Melville 1975). The contours are at 1 cm intervals.

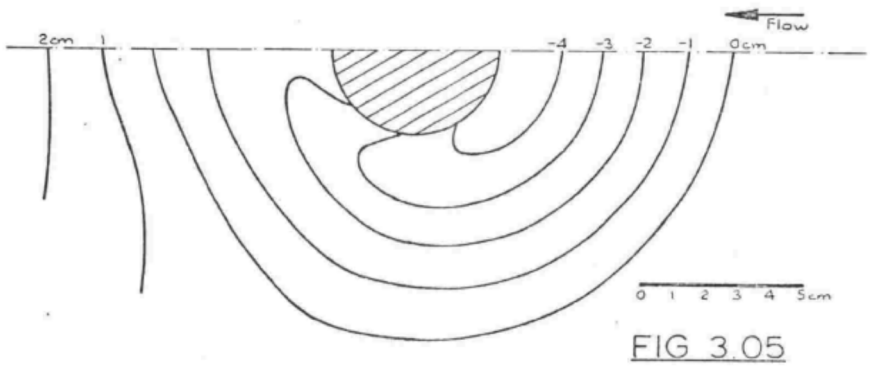

Figure B.1 Contour plot of the resulting intermediate scour hole after a half hour of flow time (Melville 1975, p. 93).

B.2 Equilibrium scour hole

Figure B.2 shows sectional elevation diagrams of the equilibrium scour hole after 2.5 hrs flow time (Melville 1975).

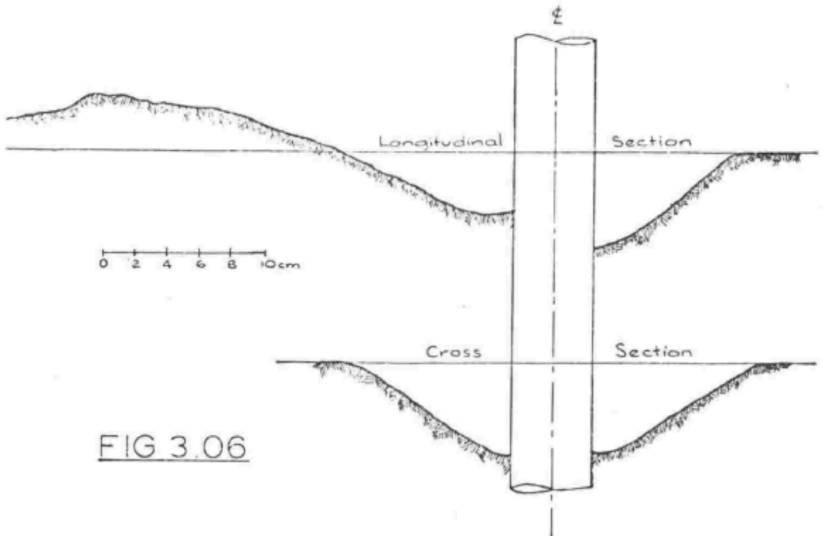

Figure B.2 Sectional elevation diagrams of the resulting equilibrium scour hole after 2.5 hrs flow time (Melville 1975, p. 94).

Figure B.3 shows a contour plot of the equilibrium scour hole after 2.5 hrs flow time (Melville 1975). The contours are at 1 cm intervals.

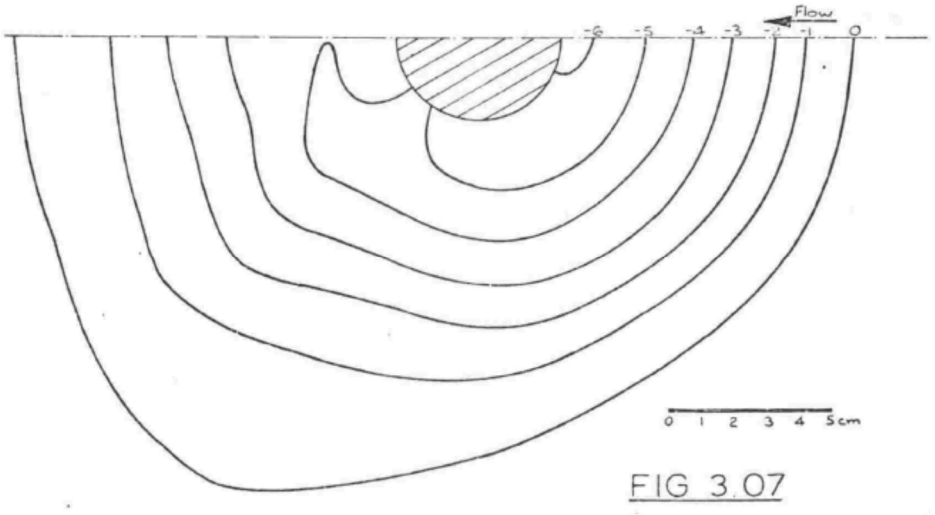

Figure B.3 Contour plot of the resulting equilibrium scour hole after 2.5 hrs flow time (Melville 1975, p. 94).

Appendix C

Empirical estimate formulae calculations

C.1 HEC-18 formula

C.1.1 Input data

C.1.2 Application of the HEC-18 formula

C.1.3 Resultant HEC-18 formula estimate

C.2 Sheppard formula

C.2.1 Input data

C.2.2 Application of the Sheppard formula

C.2.3 Critical velocity for sediment motion

C.2.4 Resultant Sheppard formula estimate

C.3 Melville formula

C.3.1 Input data

C.3.2 Critical flow conditions

C.3.3 Application of the Melville formula

C.3.4 Resultant Melville formula estimate

C.1 HEC18 formula

C.1.1 Input data

Input parameter variables for the model are:

flow depth, y_1 = 0.150 m;

pier width (diameter) normal to flow, a = 0.0508 m;

mean stream flow velocity, V_1 = 0.25 m s^{-1}; and

gravitational acceleration, g = 9.81 m s^{-2}.

C.1.2 Application of the HEC-18 formula

The HEC-18 formula (Arneson et al. 2012), described as (2.6) in Chapter 2, for estimation of maximum equilibrium local scour depth (y_s) is:

$$\frac{y_s}{y_1} = 2.0\, K_1 K_2 K_3 \left(\frac{a}{y_1}\right)^{0.65} Fr_1^{0.43}\,, \qquad \text{(C.1)}$$

Application to calculations for this project follow the procedure described in the cited journal document. The correction factors are explained and evaluated below.

The K_1 correction factor

The K_1 correction factor is for pier nose shape and given as 1.0 for a rounded nose or cylindrical pier (Arneson et al. 2012, p. 7.4).

The K_2 correction factor

The K_2 correction factor is for angle of attack of flow and is taken as 1.0 for an angle of zero degrees when the pier is aligned with flow direction (Arneson et al. 2012, p. 7.4).

The K_3 correction factor

The K_3 correction factor is for bed condition and is taken as 1.0 for clear-water scour conditions (Arneson et al. 2012, p. 7.5).

The Froude number

The Froude number (Fr_1) is calculated as:

$$Fr_1 = {V_1}/{(gy_1)^{0.5}} \quad , \tag{C.2}$$

$$= {0.25}/{(9.81 \times 0.15)^{0.5}} \quad ,$$

$$= 0.20609 \quad \text{(Dimensionless).}$$

C.1.3 Resultant HEC-18 formula estimate

$$y_s = y_1 \times 2.0\, K_1 K_2 K_3 \left(\frac{a}{y_1}\right)^{0.65} Fr_1^{0.43} \quad , \tag{C.3}$$

$$= 0.150 \times 2.0 \times 1.0 \times 1.0 \times 1.1 \left(\frac{0.0508}{0.150}\right)^{0.65} (0.20609)^{0.43} \quad ,$$

$$= 0.0828 \quad \text{m.}$$

C.2 Sheppard formula

C.2.1 Input data

Input parameter variables for the model are:

median diameter of sediment particles, D_{50} = 0.000385 m;

specific gravity of sediment, sg = 2.65;

gravitational acceleration, g = 9.81 m s^{-2};

kinematic viscosity of water, v = 1.003E-6 m^2 s^{-1};

flow depth, y_0 = 0.150 m;

mean stream flow velocity, V = 0.25 m s^{-1}; and

effective pier diameter, D^* = 0.0508 m.

C.2.2 Application of the Sheppard formula

The Sheppard equation (FDOT 2005, eq. 3.4) for clear-water scour, described as (2.7) in Chapter 2, for estimation of maximum equilibrium local scour depth (y_s) is:

$$\frac{y_s}{D^*} = 2.5 \tanh\left[\left(\frac{y_0}{D^*}\right)^{0.4}\right]\left\{1 - 1.75\left[\ln\left(\frac{V}{V_c}\right)\right]^2\right\}\left[\frac{{D^*}/{D_{50}}}{0.4\left({D^*}/{D_{50}}\right)^{1.2} + 10.6\left({D^*}/{D_{50}}\right)^{-0.13}}\right] \quad \text{(C.4)}$$

Critical velocity (V_c) and other pre-requisite parameter values were determined in accord with the instructions on page 3.10 of the Florida Bridge Scour Manual (FDOT 2005, p. 3.10). The clear-water scour equation is applicable for flow velocity ratios of $0.47 < V/V_c < 1.0$, where V_c must be calculated as specified in the manual.

C.2.3 Critical velocity for sediment motion

$$d_* = D_{50}\left[{(sg-1)g}/{v^2}\right]^{1/3} \quad , \qquad \text{(C.5)}$$

$$= 0.000385\left[{(2.65-1)\times 9.81}/{(1.003\times 10^{-6})^2}\right]^{1/3} \quad ,$$

= 9.7195 (Dimensionless).

$$\Theta_c = 0.0023d_* - 0.000378d_* \ln(d_*) + {0.23}/{d_*} - 0.005 \quad , \qquad \text{(C.6)}$$

$$= 0.02235485 - 0.008355103 + 0.023663768 - 0.005 \quad ,$$

= 0.03266 (Dimensionless).

$$U_{*c} \equiv \sqrt{\frac{\tau_c}{\rho}} = \sqrt{\Theta_c(sg-1)gD_{50}} \quad , \qquad \text{(C.7)}$$

$$= \sqrt{0.03266\times(2.65-1)\times 9.81\times 0.000385} \quad ,$$

= 0.01427 m/s.

$$k_s \equiv 5D_{50} \quad \text{for } D_{50} < 0.6 \text{ mm} \quad , \qquad \text{(C.8)}$$

= 5 x 0.000385 ,

= 0.001925 m.

$$Re_c = {U_{*c}k_s}/{\nu} \quad , \tag{C.9}$$

$$= \frac{0.01427 \times 0.001925}{1.003 \times 10^{-6}} \quad ,$$

= 27.388 (Dimensionless).

$$z_0 = k_s \times 10^{-3}\left[-6 + 2.85Re_c - 0.58Re_c \ln(Re_c) + 0.002Re_c^2 + \frac{111}{Re_c}\right] \quad , \tag{C.10}$$

$$= \frac{0.001925}{1000}[-6 + 78.0558 - 52.581 + 1.5002 + 4.0529] \quad ,$$

= 4.8179 x 10^{-5} m.

$$V_c = 2.5U_{*c} \ln\left(\frac{y_0}{2.72z_0}\right) \quad , \tag{C.11}$$

$$= 2.5 \times 0.01427 \times \ln\left(\frac{0.150}{2.72 \times 4.8179 \times 10^{-5}}\right) \quad ,$$

= 0.2513 m/s.

$${V}/{V_c} = {0.250}/{0.2513} = 0.995 \quad . \tag{C.12}$$

C.2.4 Resultant Sheppard formula estimate

Maximum equilibrium local scour depth is calculated as (FDOT 2005, eq. 3.4):

$$\frac{y_s}{D^*} = 2.5 \tanh\left[\left(\frac{y_0}{D^*}\right)^{0.4}\right]\left\{1 - 1.75\left[\ln\left(\frac{V}{V_c}\right)\right]^2\right\}\left[\frac{{D^*}/{D_{50}}}{0.4\left({D^*}/{D_{50}}\right)^{1.2} + 10.6\left({D^*}/{D_{50}}\right)^{-0.13}}\right]$$

(C.13)

$$y_s = 0.0508 \times 2.5 \tanh\left[\left(\frac{0.150}{0.0508}\right)^{0.4}\right]\left\{1 - 1.75\left[\ln\left(\frac{0.250}{0.2513}\right)\right]^2\right\} \ldots$$

$$\ldots \left[\frac{{0.0508}/{0.000385}}{0.4\left({0.0508}/{0.000385}\right)^{1.2} + 10.6\left({0.0508}/{0.000385}\right)^{-0.13}}\right]$$

$$= 0.1049 \quad \text{m.}$$

C.3 Melville formula

C.3.1 Input data

Input parameter variables for the model are:

water density, $\rho = 1000$ kg m^{-3};
sand density, $\rho_s = 2650$ kg m^{-3};
mean sand grain diameter, $d_{50} = 0.385$ mm;
gravitational acceleration, $g = 9.81$ m s^{-2};
flow depth, $y_0 = 0.150$ m;
bed slope, $S_0 = 0.0001$ m m^{-1};
mean stream flow velocity, $U = 0.25$ m s^{-1}; and
pier width (diameter) normal to flow, $D = 0.0508$ m.

Melville (1975) considered the sand in the original physical experiment to be fairly well graded; a distribution ranging between 0.1 and 1.0 mm diameter was displayed in a graph. Geometric standard deviation (σ_g) of grain size was not given but can be found from an estimate of 84th percentile grain size (d_{84}) equals 0.65 mm, read from the graph, used in the equation (Melville & Sutherland 1988, p. 1211):

$$\sigma_g = {}^{d_{84}}/_{d_{50}} \quad , \qquad \text{(C.14)}$$
$$= {}^{0.65}/_{0.385} \quad ,$$
$$= 1.688 \quad .$$

C.3.2 Critical flow conditions

A preliminary step is required to determine:

- critical friction velocity (u_{*c}) and critical mean stream flow velocity (U_c) for the nominated d_{50} grain size; and
- critical armoured friction velocity (u_{*ca}) and critical mean armoured stream flow velocity (U_a) for the maximum bed armouring condition.

The Shields diagram is indirectly used to determine the critical friction velocity, at the threshold of motion, for the given grain size. The Shields diagram requires values of entrainment function and shear Reynolds number as inputs, however formulas for both of these values also require the unknown critical friction velocity as an input. Solution requires an initial estimate followed by an iterative refinement process. The correct friction velocity solution is confirmed when co-ordinate values of entrainment function and shear Reynolds number plot exactly on the Shields function line.

Melville & Sutherland (1988) suggest an alternative estimation method whereby a chart of critical friction velocity versus a range of grain sizes is derived from the Shields diagram. This requires reading pairs of entrainment value and shear Reynolds number from the Shields function and solving their respective formulas as simultaneous equations, for both grain diameter and critical shear velocity. Plotted results allow a close estimate of the critical shear velocity to be directly read from the chart for any grain size in the plotted range. The chart must be specifically prepared using densities and fluid viscosity particular to the given situation. Such a chart (Figure C.1) has been prepared to suit this research project. The chart shows critical shear velocity estimated as 0.015 m/s for a grain size of 0.385 mm.

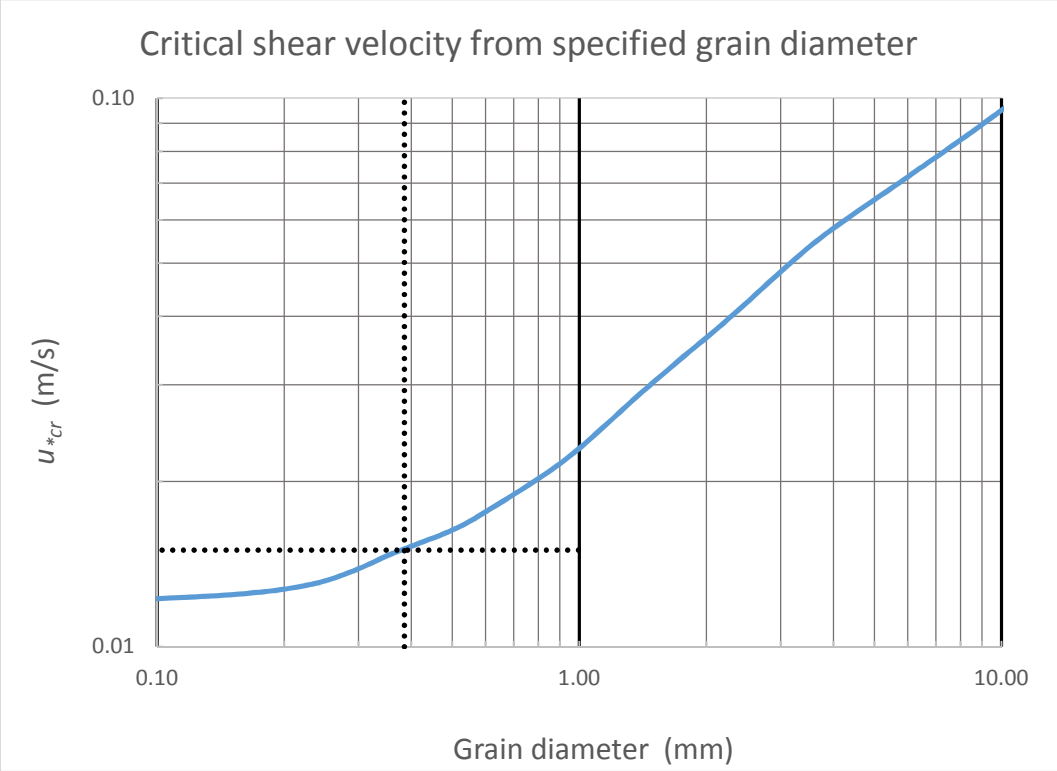

Figure C.1 Chart prepared for estimation of critical shear velocity at threshold conditions; demonstrated for the 0.385 mm nominated grain size.

Melville & Sutherland (1988, eq. 2) indicate the critical shear velocity can be converted to a critical mean stream flow velocity using the formula:

$$U_c = u_{*c} \times 5.75 \log\left(5.53 \frac{y_0}{d_{50}}\right) \qquad \text{(C.15)}$$

$$= 0.015 \times 5.75 \log\left(5.53 \frac{0.15}{0.000385}\right)$$

$$= \ 0.288 \ \ \text{m s}^{-1}.$$

For the bed armouring condition it is assumed the finer grain sizes will have been washed away so the mean size of the remaining grains (d_{50a}) will be larger than it was for the original grain distribution. The value of d_{50a} is calculated from the largest possible armouring grain size (d_{max}). The value of d_{max} is calculated from (Melville & Sutherland 1988, eq. 3):

$$d_{max} = \sigma_g^m d_{50} \ , \qquad \text{(C.16)}$$

using a value of exponent *m* from Table 1 of the cited reference.

The value of d_{50a} is calculated as (Melville & Sutherland 1988, p. 1212):

$$d_{50a} = {}^{d_{max}}/_{1.8}\,, \qquad \text{(C.17)}$$

$$= \frac{1.688^{2.34} \times 0.385}{1.8}$$

$$= \quad 0.728 \quad \text{mm.}$$

Referring to the chart of Figure C.1 this gives a u_{*ca} of 0.019 m/s. The value of U_{ca} is calculated from (C.2) as 0.344 m/s. The value of U_a is calculated as (Melville & Sutherland 1988, p. 1212):

$$U_a = 0.8U_{ca} \qquad \text{(C.18)}$$

$$= \quad 0.267 \quad \text{m/s.}$$

The value of U_a has been calculated for the most severe case of bed armouring but the value attained is less than U_c. This is an unrealistic result therefore U_a is taken as equal to U_c.

C.3.3 Application of the Melville formula

The Melville formula (Melville & Sutherland 1988, eq. 7), described as (2.8) in Chapter 2, for estimation of maximum equilibrium local scour depth (d_s) is:

$$\frac{d_s}{D} = K_I K_y K_d K_\sigma K_s K_\alpha \quad . \qquad \text{(C.19)}$$

Application to calculations for this project follow the procedure described in the cited journal document. The *K* correction factors are explained and evaluated below.

The K_I correction factor

The K_I correction factor is a flow intensity factor with a maximum value of 2.4, however it may be reduced in particular circumstances (Melville & Sutherland 1988).

The ratio of mean stream flow velocity to critical mean stream flow velocity is an indication of flow intensity; it is used as the basis of the K_I correction factor. An additional term for critical armoured mean stream flow velocity (U_a) accounts for bed armouring when sediment is non uniform. For this project a ratio of U/U_c <1 indicates clear water conditions exist, therefore no general scouring occurs and no sediment is transported from further upstream. Consequently, bed armouring does not occur and the U_a term is taken to be equal to the U_c term.

The K_I correction factor is calculated as (Melville & Sutherland 1988, eq. 10a):

$$K_I = 2.4\left|\frac{U-(U_a-U_c)}{U_c}\right| \text{, where } \frac{U-(U_a-U_c)}{U_c} < 1 \qquad \text{(C.20)}$$

$$= 2.4\left|\frac{0.25-(0.288-0.288)}{0.288}\right|$$

$$= \ 2.083$$

The K_y correction factor

The K_y correction factor is a flow depth factor and is given as 1.0 when the ratio y_0/D is greater than 2.6 (Melville & Sutherland 1988, p. 1214). The ratio y_0/D is 2.95 in this project.

The K_d correction factor

The K_d correction factor is a sediment size factor and is given as 1.0 when the ratio D/d_{50} is greater than 25 (Melville & Sutherland 1988, p. 1215). The ratio D/d_{50} is 132 in this project.

The K_σ correction factor

The K_σ correction factor is a sediment gradation factor and is always given as 1.0 because its effects are accounted for by the U_a term within the K_I factor (Melville & Sutherland 1988, p. 1219).

The K_s correction factor

The K_s correction factor is a pier shape factor and is given as the reference value of 1.0 for piers of circular cross-section (Melville & Sutherland 1988, p. 1220).

The K_α correction factor

The K_α correction factor is a pier alignment factor for piers not aligned with the stream flow direction. The reference value of 1.0 is given for circular cross-section piers because they have no particular orientation (Melville & Sutherland 1988, p. 1220).

C.3.4 Resultant Melville formula estimate

Maximum equilibrium local scour depth is calculated as (Melville & Sutherland 1988, eq. 11):

$$d_s = K_I K_y K_d K_s K_\alpha D \quad . \qquad \text{(C.21)}$$
$$= 2.083 \times 1.0 \times 1.0 \times 1.0 \times 1.0 \times 0.0508$$
$$= \ 0.1058 \ \ \text{m.}$$

Note: the K_σ factor is omitted because it is always given as a factor of 1.0 and is therefore inconsequential.

Appendix D

Model diagrams

D.1 Domain diagram

D.2 Result diagrams

D.2.1 2-D results

D.2.2 3-D results

D.1 Domain diagram

Figure D.1 shows a full length view of the model domain. All the component stages can be seen, including the long turbulent inflow stage which is suppressed in most other model diagrams.

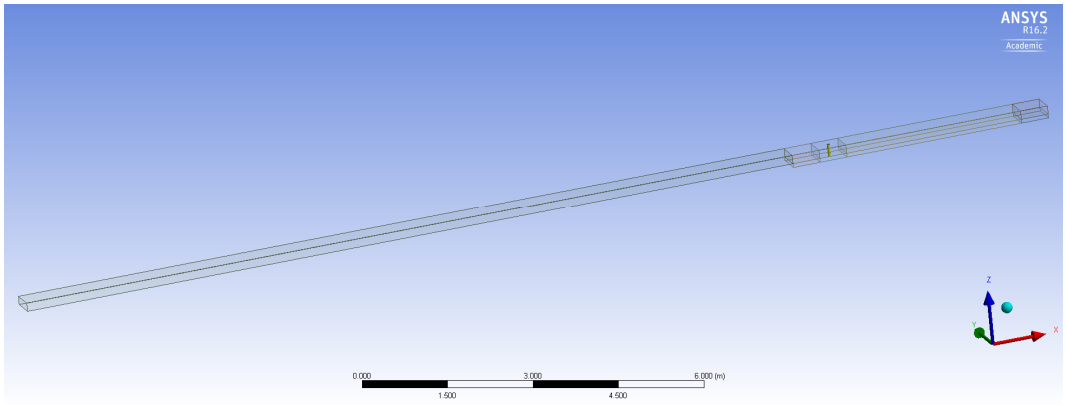

Figure D.1 A full length view of the model domain, showing all the component stages.

D.2 Result diagrams

D.2.1 2-D results

Figures D.2 and D.3 show the velocity profile in a horizontal plane around the cylindrical pier and the new slotted pier respectively. Both diagrams include the full length of the outflow stage and show the velocity profile stabilising downstream of the pier.

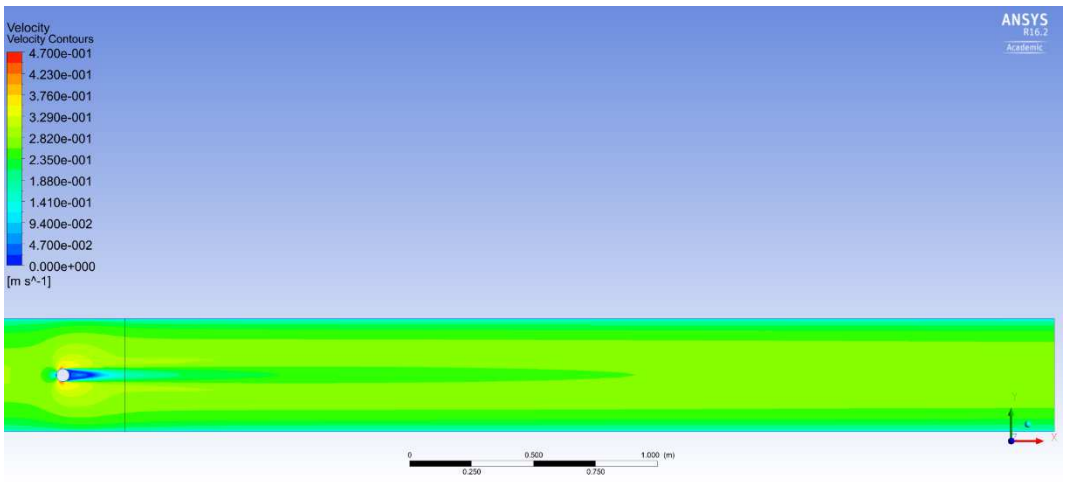

Figure D.2 Velocity profile around the cylindrical pier, and stabilising as it flows downstream to the outlet.

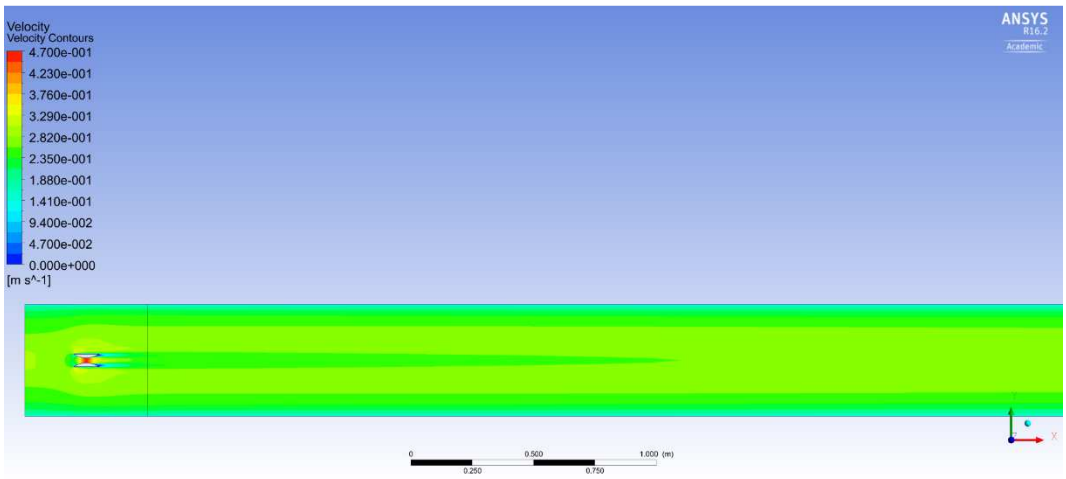

Figure D.3 Velocity profile around the new slotted pier, and stabilising as it flows downstream to the outlet.

D.2.2 3-D results

Figures D.4 to D.7 show an isosurface at a range of different volume fractions. These results are from an early trial and are showing different surface representations at the same point in time. They suggest some degree of interpretation is required to determine where the simulated sand surface is actually located. At lower volume fractions the surface appears to be unblemished whereas at the highest possible volume fraction it appears to have incurred the most erosion.

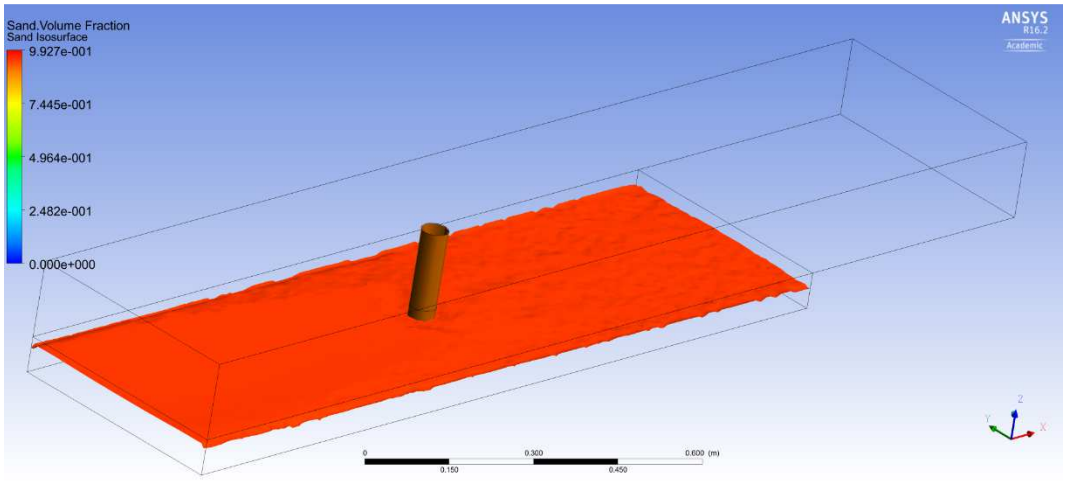

Figure D.4 An isosurface at 0.950 sand volume fraction.

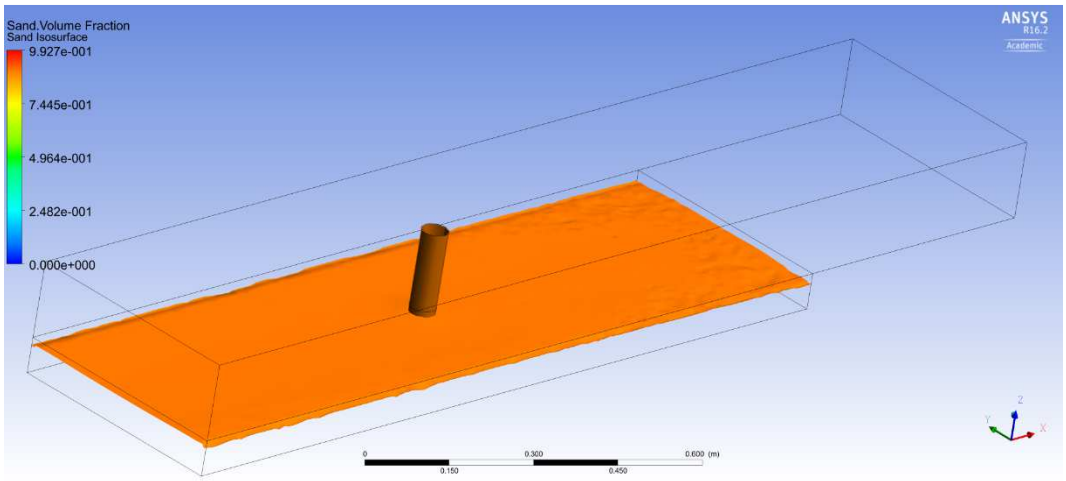

Figure D.5 An isosurface at 0.90 sand volume fraction.

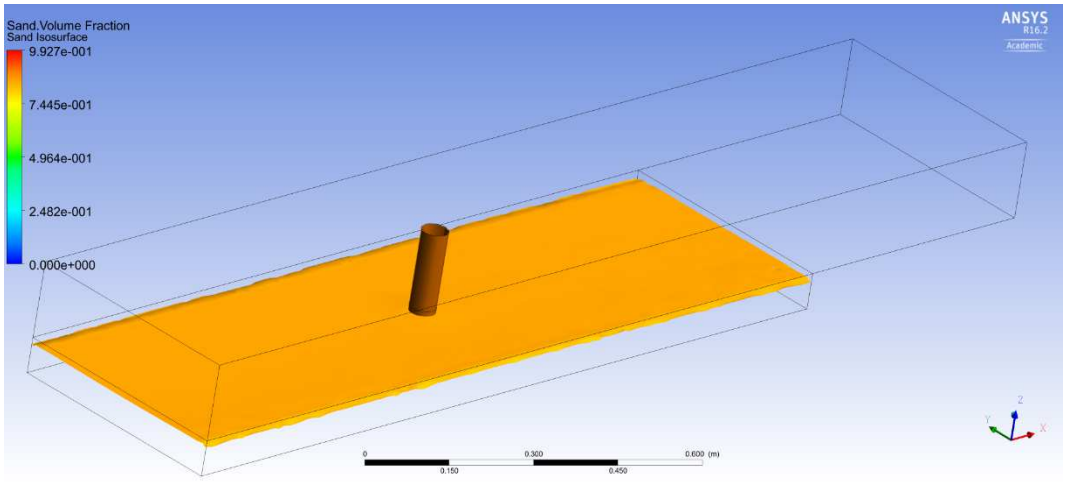

Figure D.6 An isosurface at 0.850 sand volume fraction.

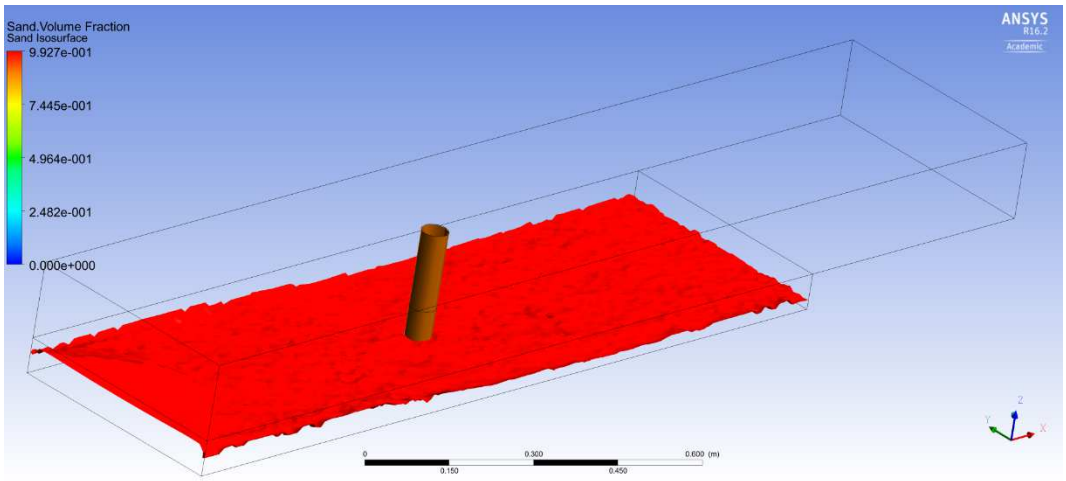

Figure D.7 An isosurface at 0.991 sand volume fraction.

Figures D.8 to D.13 show an isosurface at a progressive range of flow times during continued running of the last cylindrical pier trial. They show a progressive increase in the degree of general scouring over the sand surface. Initially there is little general scouring and some suggestion of localised scouring, however this is wiped

out over a period of time. The isosurfaces were all at a volume fraction of 0.62 except for the last one. At 20 seconds run time a surface at 0.62 volume fraction no longer existed.

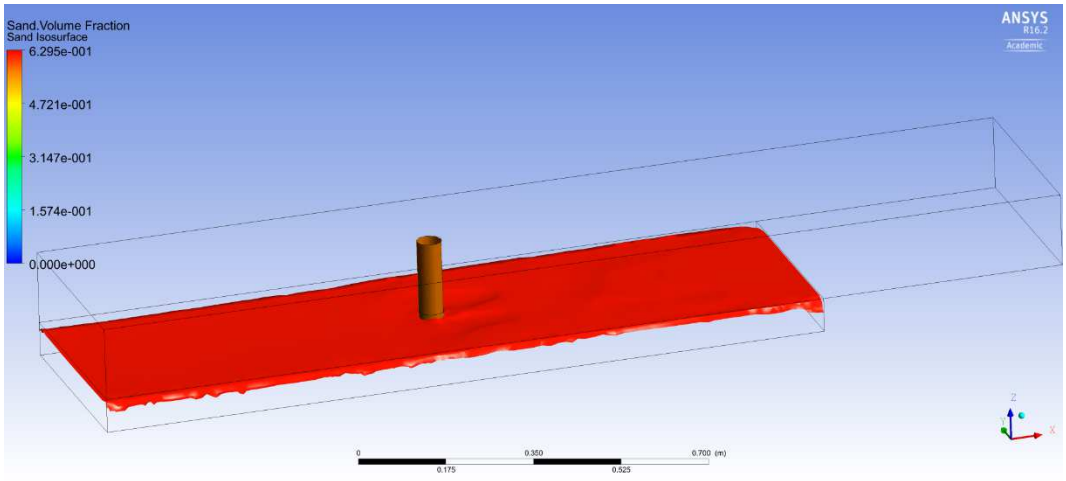

Figure D.8 An isosurface at 0.62 sand volume fraction after 3.52 seconds flow time. It shows a suggestion of localised scouring to the sides and behind the pier, with very little generalised scouring.

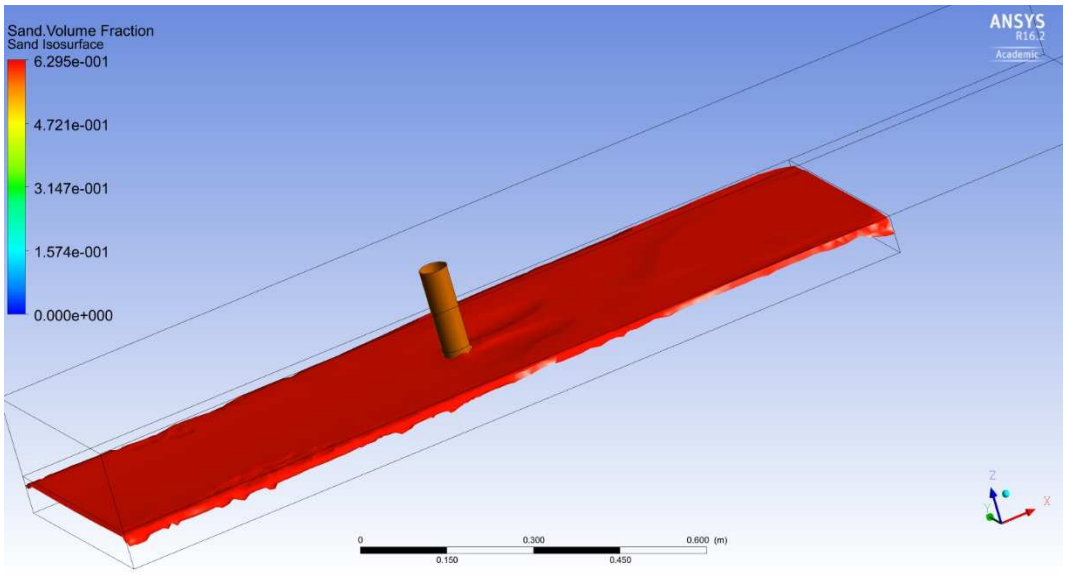

Figure D.9 An isosurface at 0.62 sand volume fraction after 4.82 seconds flow time. Small areas of generalised scouring are beginning to appear just back from the inlet.

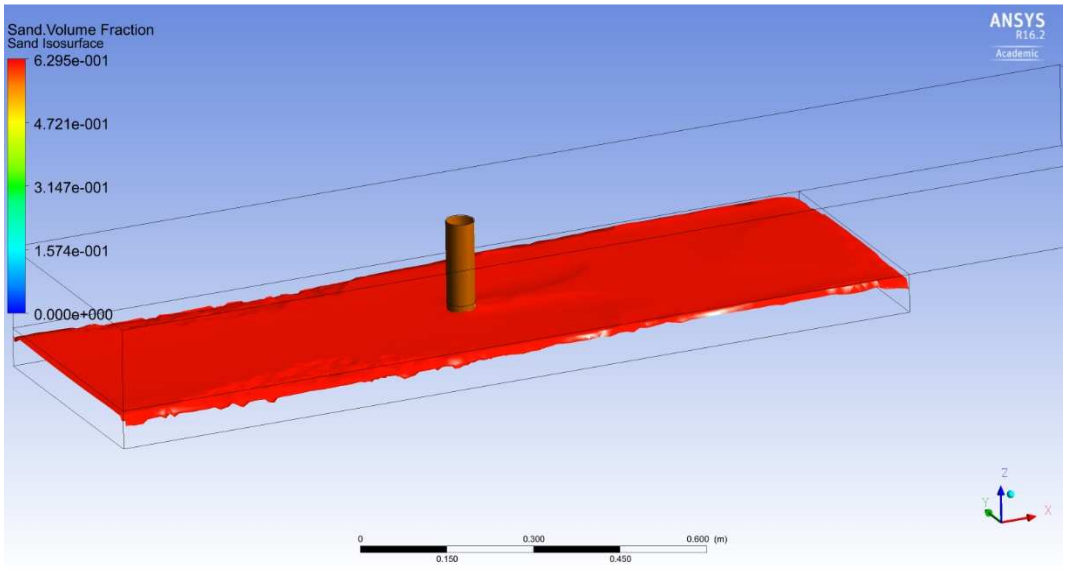

Figure D.10 An isosurface at 0.62 sand volume fraction after 8.0 seconds flow time. Generalised scouring is becoming more prominent just back from the inlet.

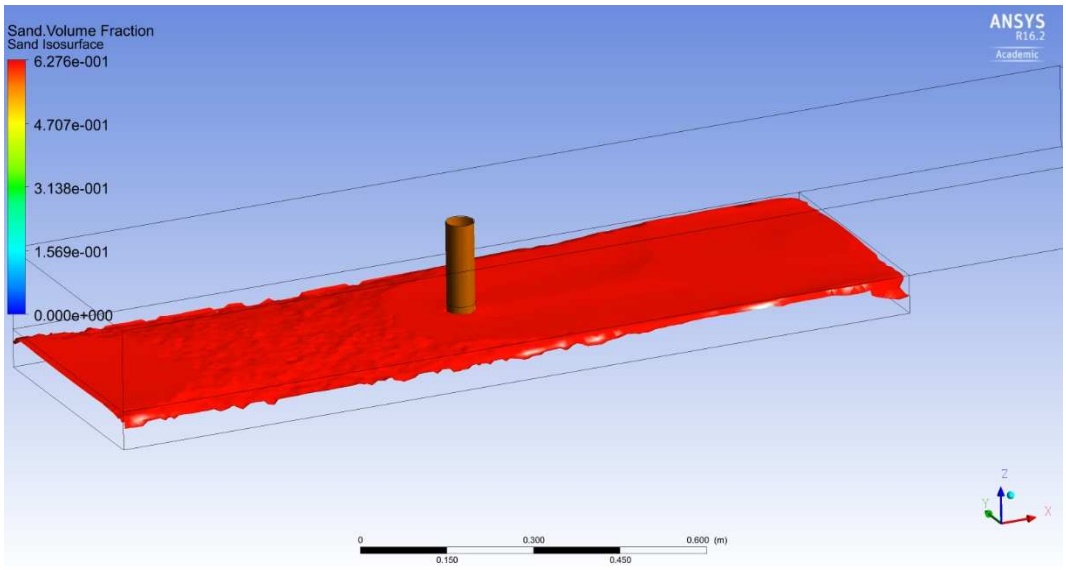

Figure D.11 An isosurface at 0.62 sand volume fraction after 12.0 seconds flow time. Generalised scouring is very prominent just back from the inlet, and localised scouring adjacent to the pier has been wiped out.

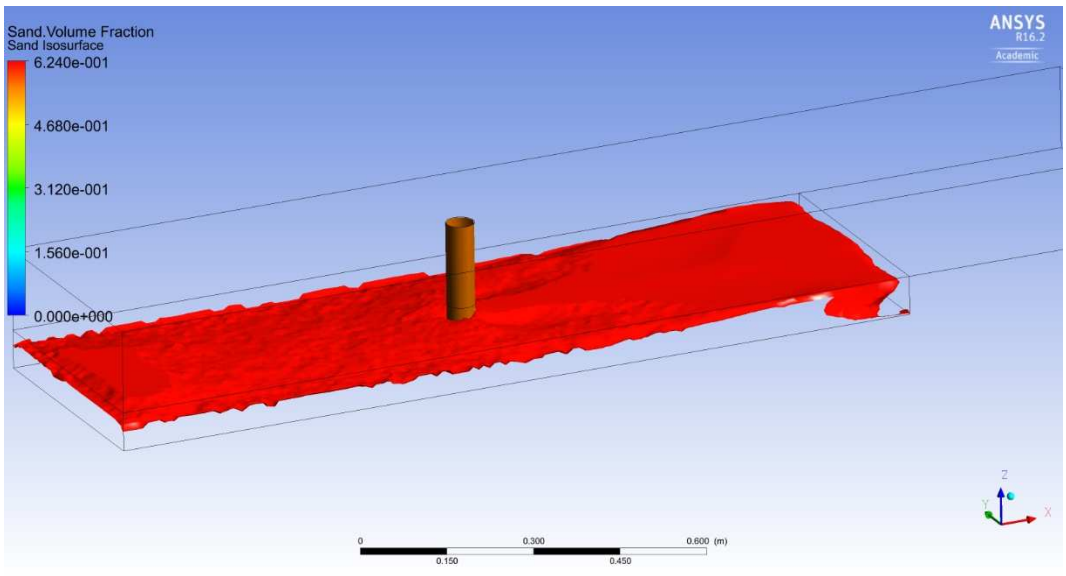

Figure D.12 An isosurface at 0.62 sand volume fraction after 16.0 seconds flow time. Generalised scouring is very prominent just back from the inlet, and localised scouring has re-emerged adjacent to the pier.

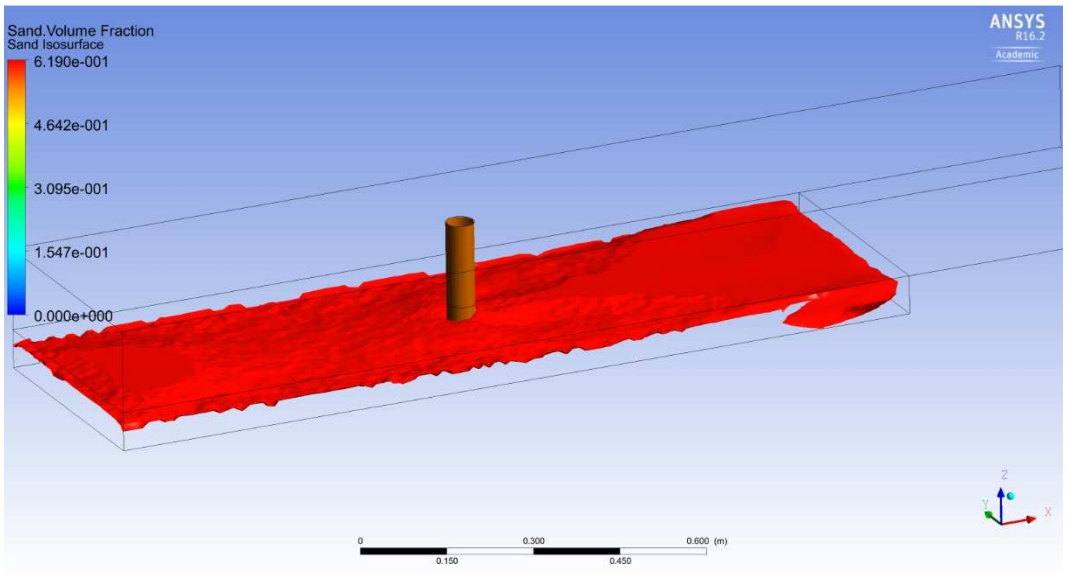

Figure D.13 An isosurface at 0.615 sand volume fraction after 20.0 seconds flow time. Results are similar to those after 16.0 seconds but generalised scouring has removed some sand volume from the entire surface area.